

Physical Properties of Irradiated Semiconductors and Ceramic Insulators

Steven J. Zinkle

Metals and Ceramics Division,
Oak Ridge National Laboratory

NATO Advanced Study Institute
32nd Course of the International
School of Solid State Physics

Erice, Sicily, Italy,

July 17-29, 2004

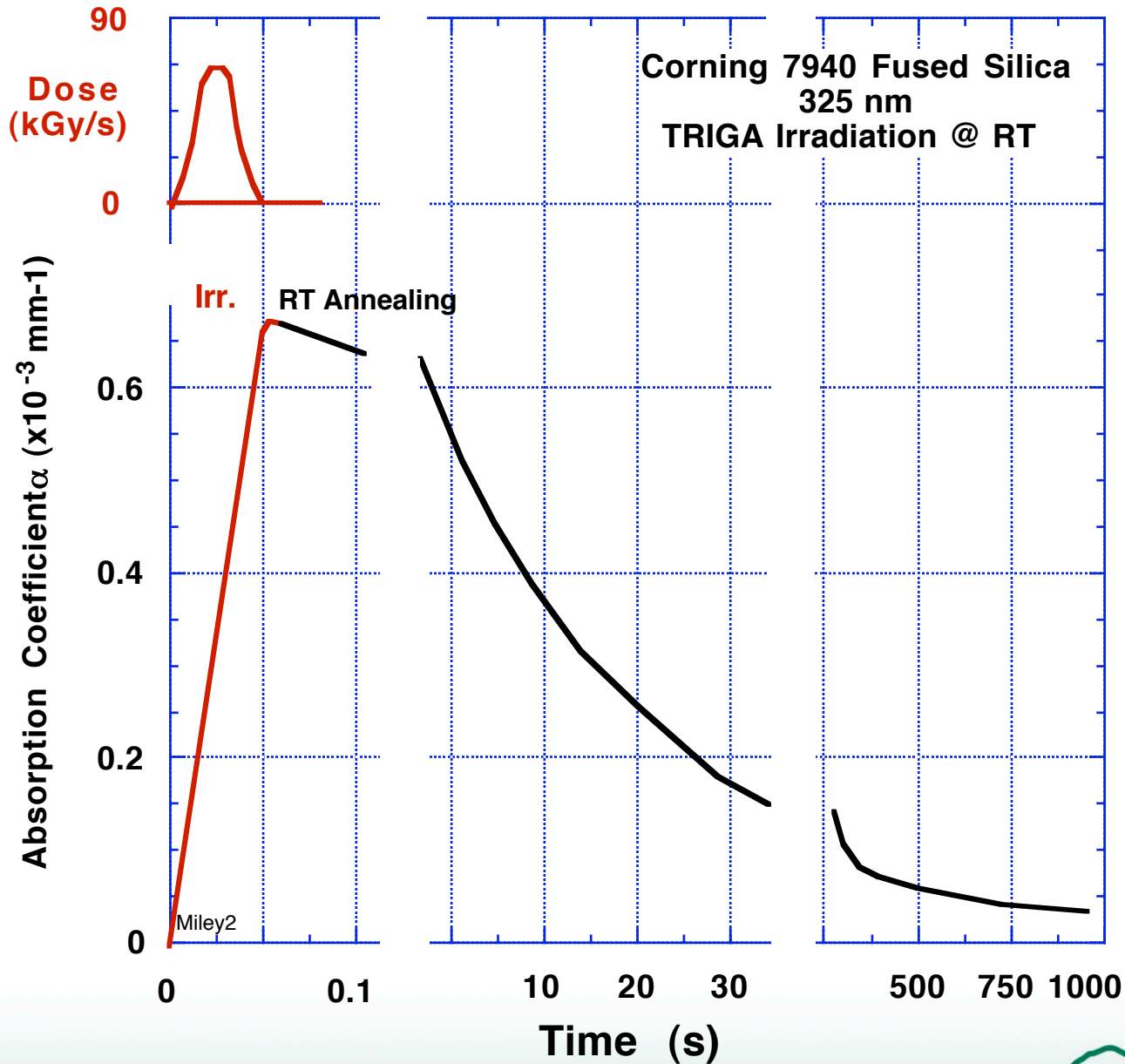
Outline

- Optical properties (defect production)
 - Effect of defect mobility on observed behavior
- Electrical conductivity
- Dielectric properties
- Thermal conductivity

Key physical property changes of irradiated metals vs. ceramic insulators and semiconductors

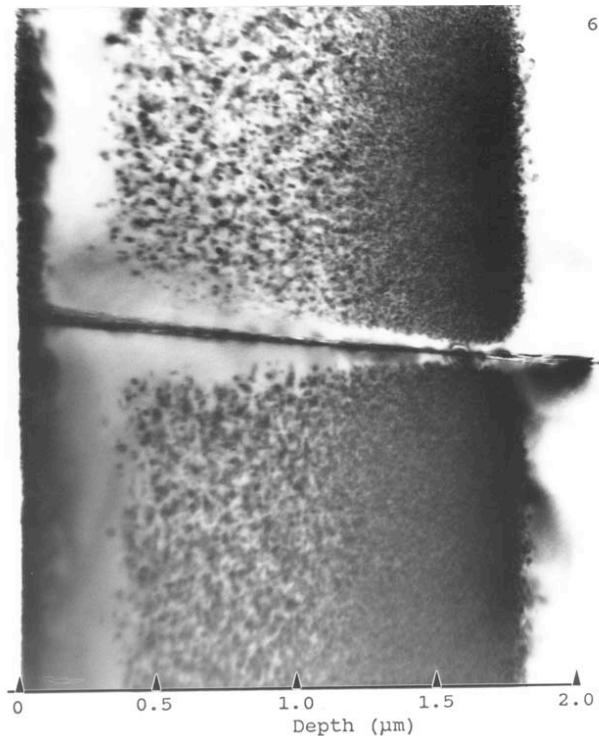
- Behavior in metals is dominated by free electrons
 - Radiation-induced changes in electrical (σ_e) and thermal conductivity (K_{th}) are useful for monitoring defects (electron-defect scattering)
 - σ_e and K_{th} are related by Lorentz ratio (Wiedemann-Franz law, $K_{th}/\sigma_e = LT$)
- Ceramic insulators and semiconductors have low free electron densities (10^{-12} to 10^{-6} per atom)
 - Ionization-induced increases in conduction electron density can cause large transient increases in electrical conductivity of insulators
 - Postirradiation σ_e properties are more strongly affected by impurity effects (n- or p- doping) than by radiation-induced vacancies and interstitials
 - Thermal conductivity is determined by phonon-defect scattering events, and can be a sensitive monitor of vacancies and interstitial defects
 - Wiedemann-Franz law is not valid for nonmetals
 - Optical properties are very sensitive monitors of radiation-induced defects (cf. lectures by Popov, Kotomin, etc.)
 - Dielectric properties (loss tangent) are also sensitive to defect concentrations in ceramic insulators

Optical absorption of neutron-irradiated SiO₂

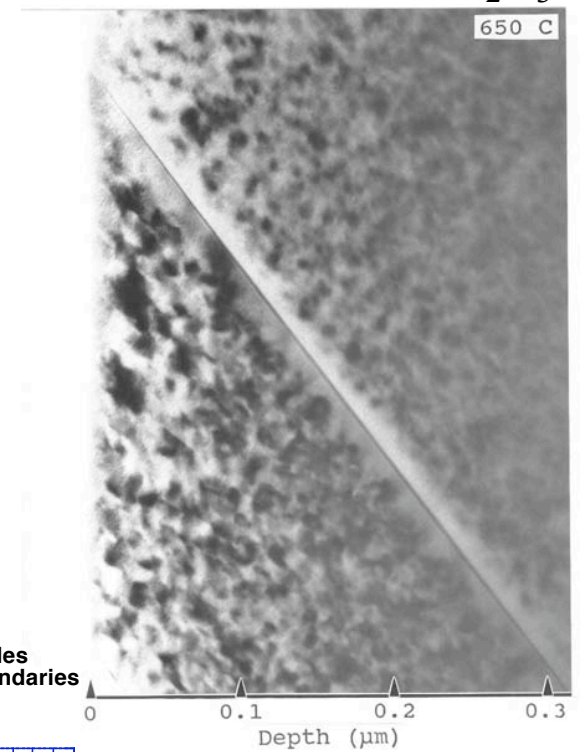


Determination of interstitial migration energies in ceramics

Defect-free zones in ion-irradiated MgAl_2O_4



Defect-free grain boundary zones in ion-irradiated Al_2O_3



- Solve steady state rate eqns:

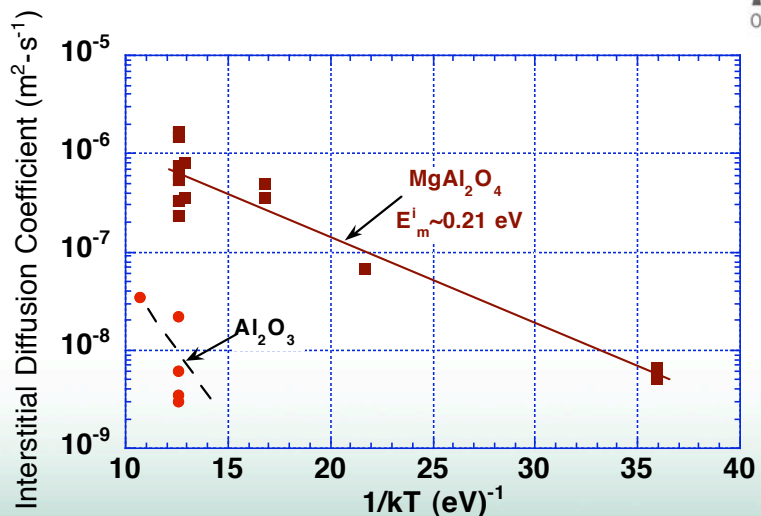
$$D_i \frac{d^2 C_i}{dx^2} - \alpha C_i C_v - D_i C_i C_s + P = 0$$

$$D_v \frac{d^2 C_v}{dx^2} - \alpha C_i C_v - D_v C_v C_s + P = 0$$

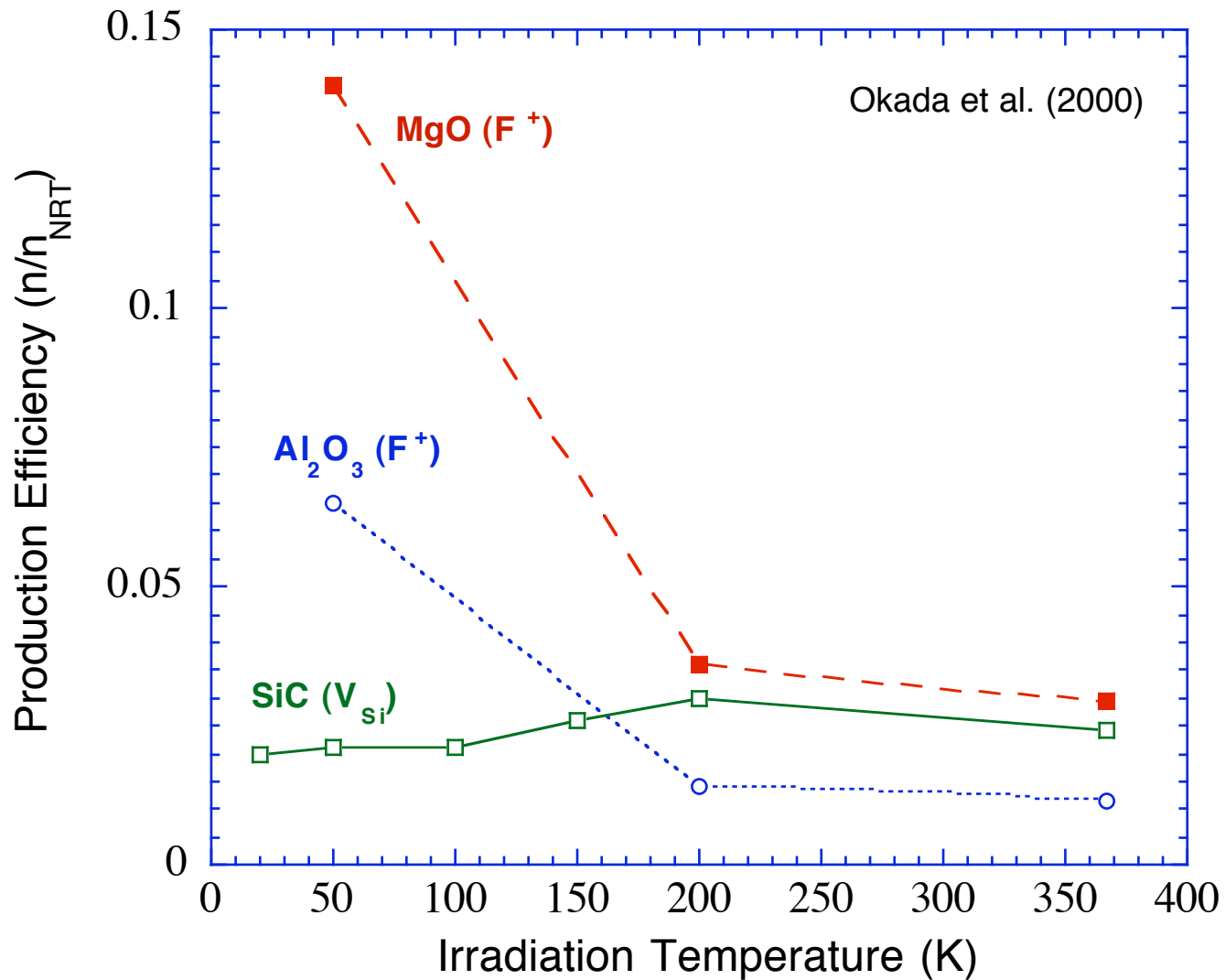
- For sink-dominant conditions ($C_s > 10^{14}/\text{m}^2$), the defect-free zone width is related to the diffusivity (D_i) and damage rate (P) by:

$$D_i = \frac{L P}{C_i^{\text{crit}} \sqrt{C_s}}$$

Interstitial Diffusion Coefficient in Ion Irradiated Oxides Determined From Defect-Free Zone Widths at Grain Boundaries

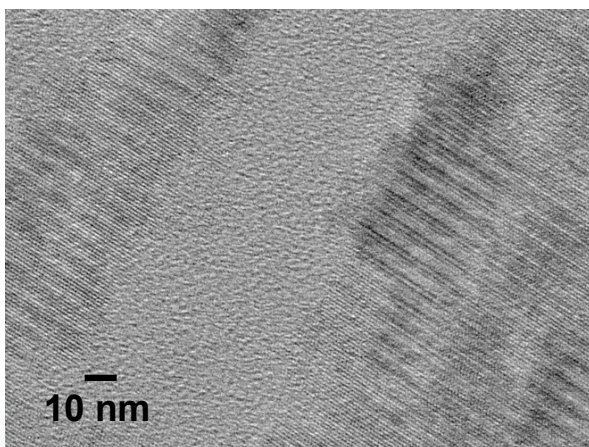
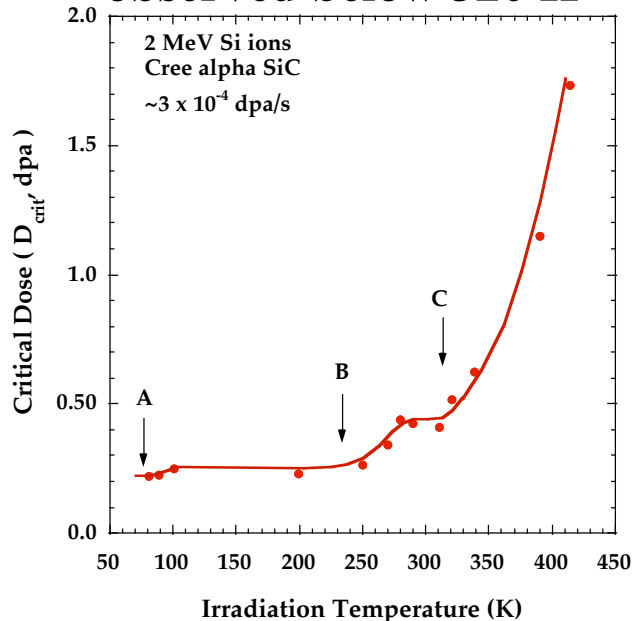


Temperature dependence of measured F center defect production

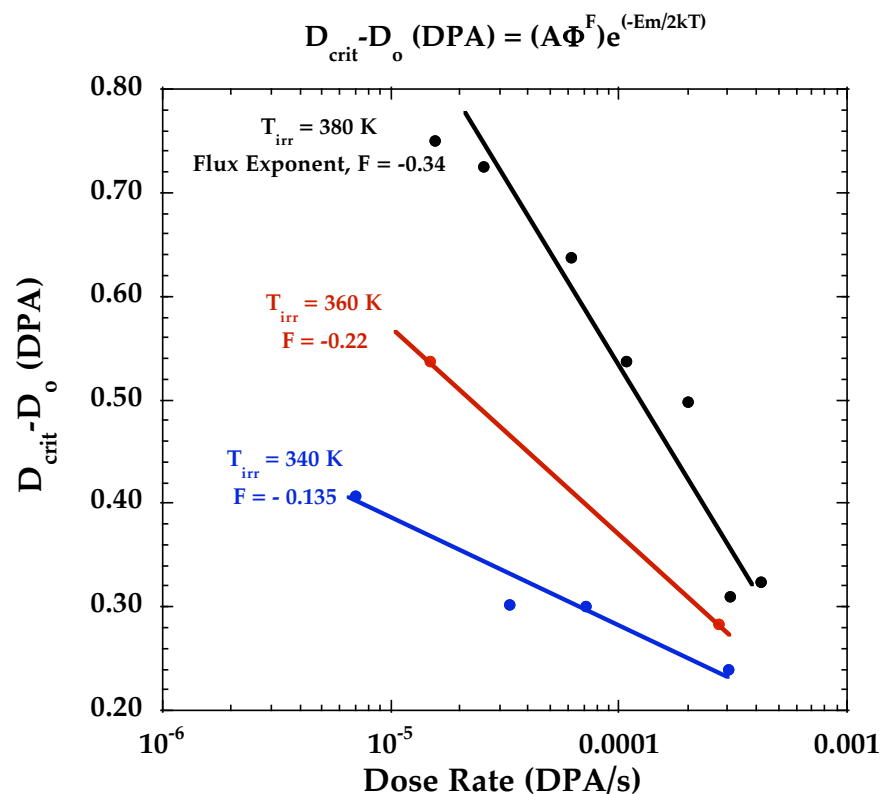


Analysis of SiC Amorphization

3 recovery substages are observed below 320 K

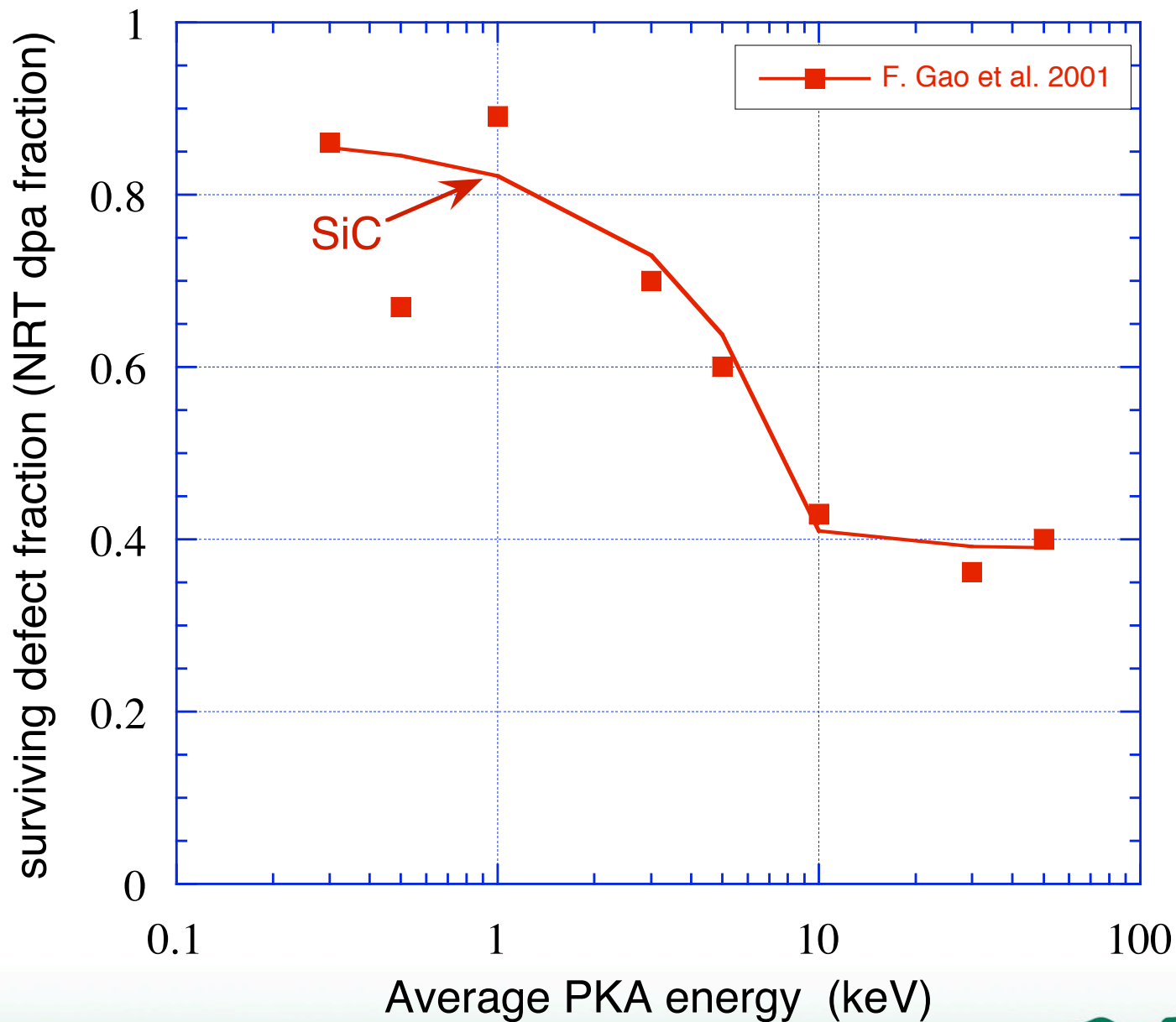


Analysis of flux dependence shows recovery substages are not associated with long range point defect migration ($F < 0.5$ up to 380 K)



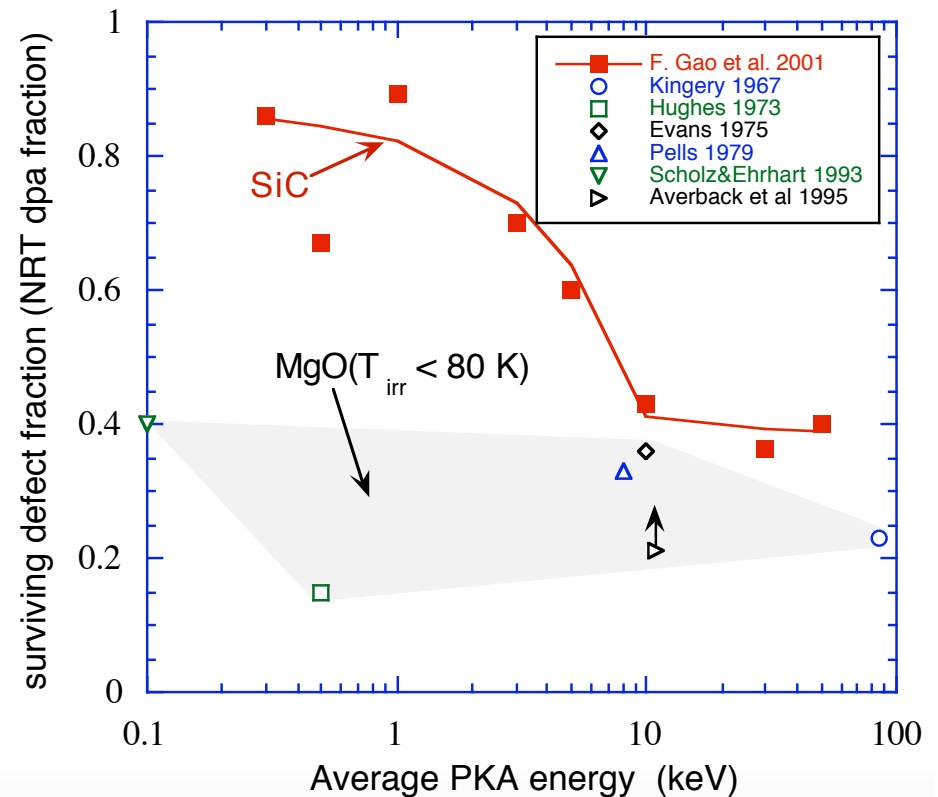
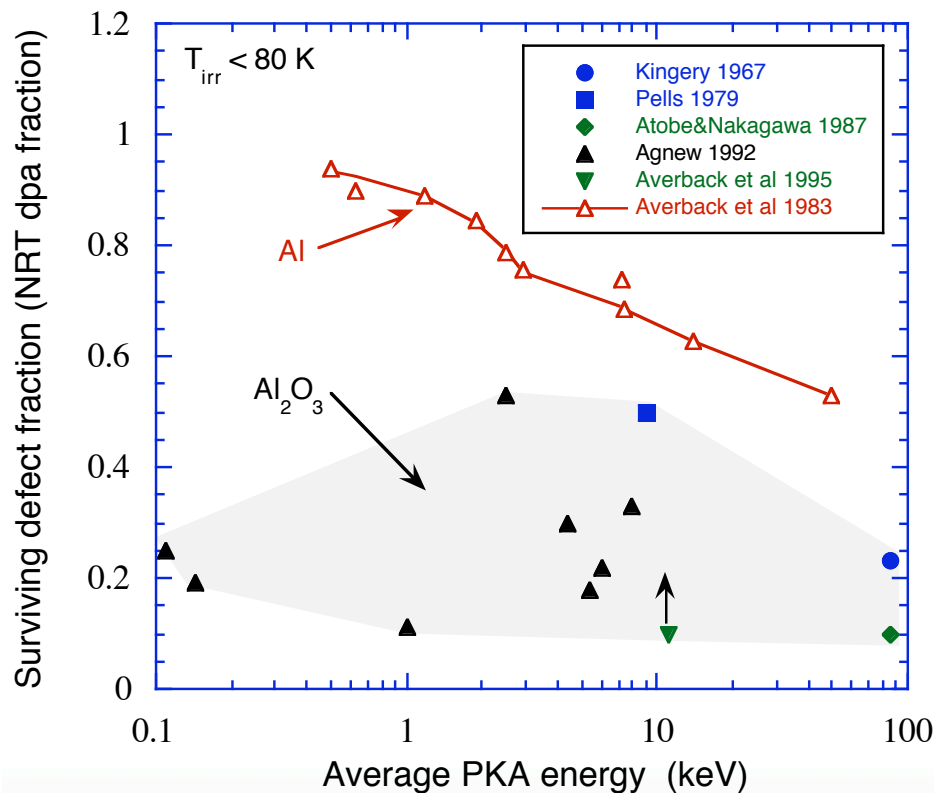
➡ Implies that both vacancies and interstitials are immobile in SiC up to 100°C (interstitials are mobile in many other ceramics at room temperature)

Total defect production efficiency



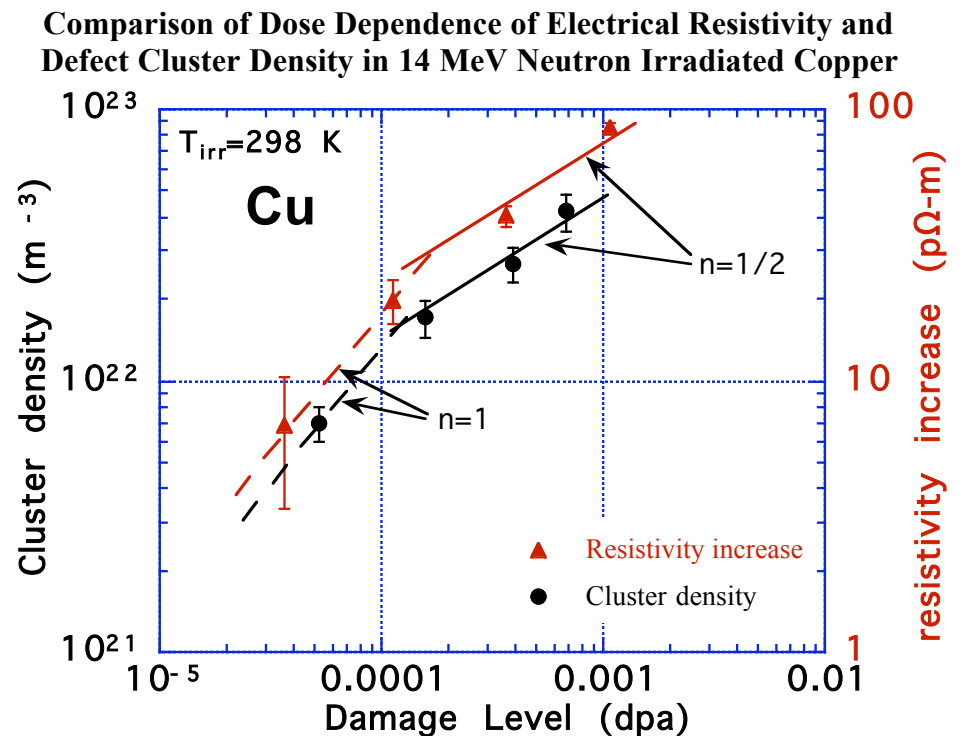
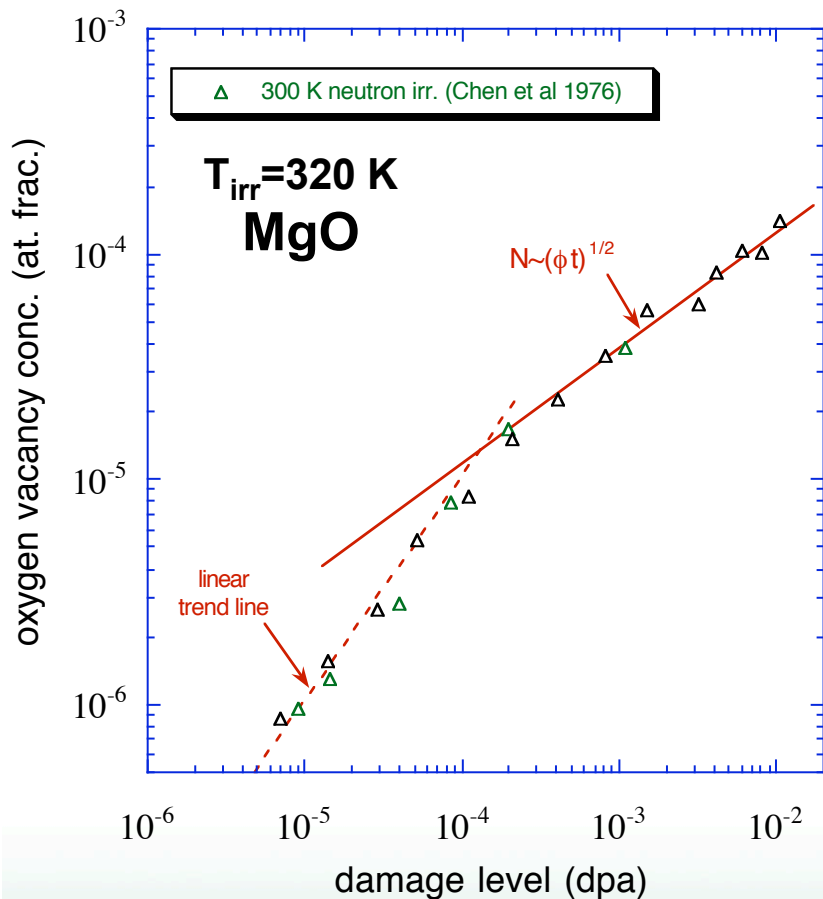
Defect Production Efficiency in Ceramics

- MD results for SiC are in general agreement with surviving defect efficiency of low-mass metals (e.g., Al)
 - Does subcascade formation occur above 10 keV in SiC?
- Al_2O_3 and MgO experimental results are suspect due to neglect of point defect migration & recovery



DEFECT PRODUCTION IN CERAMICS

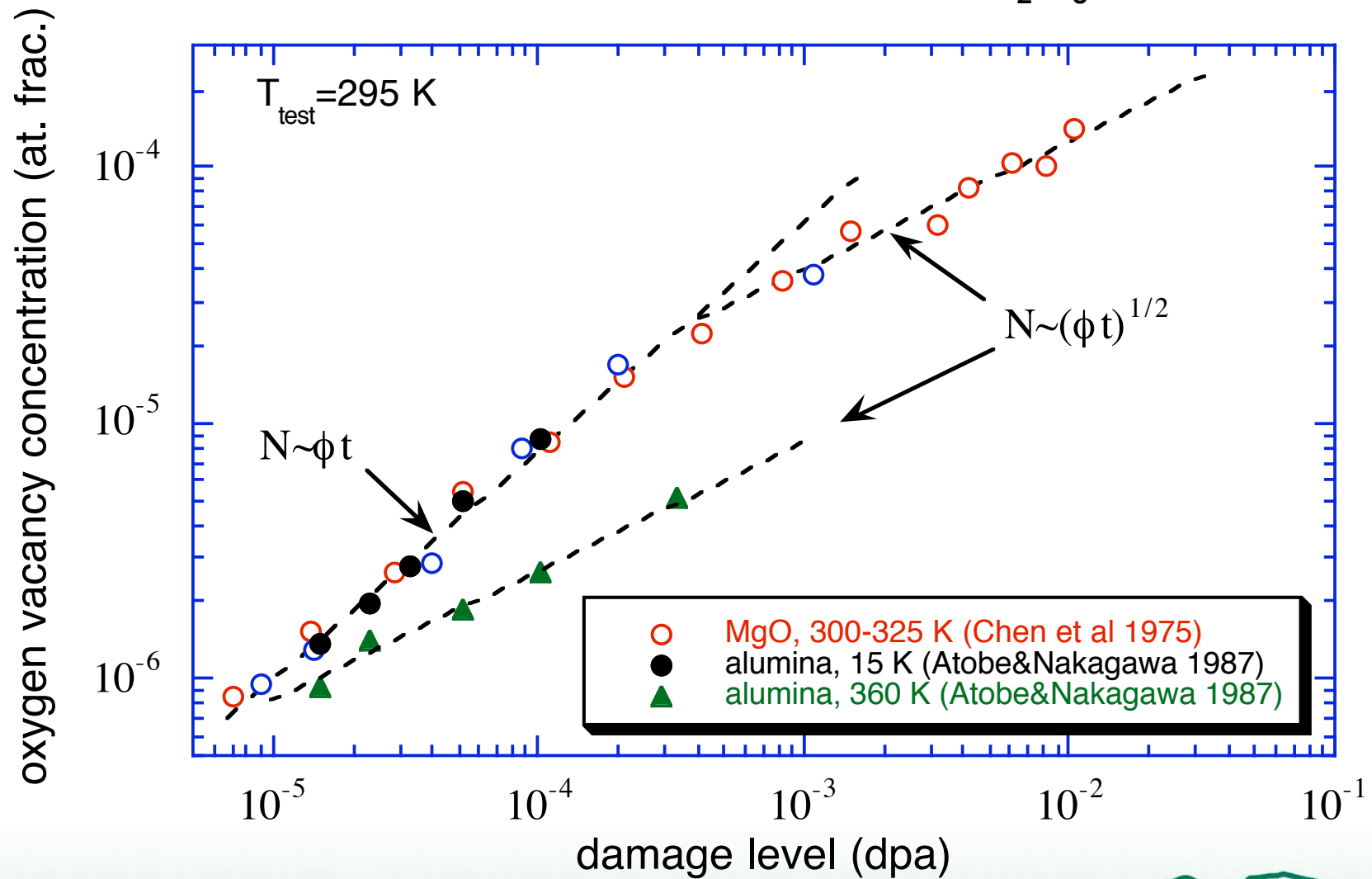
- Transition from linear to square root defect accumulation behavior is a characteristic feature of any pure material irradiated at temperatures where point defects are mobile
 - Location of transition is dependent on purity and recombination cross-section



• Data analysis indicates freely migrating interstitial fraction is $f_i \sim 11\%$ dpa_{NRT} (good agreement with MD)

DEFECT PRODUCTION IN CERAMICS

F center accumulation in neutron irradiated MgO and Al₂O₃



Ionizing Radiation can induce myriad effects in ceramics

- **Defect annealing and coalescence (ionization-induced diffusion)**
 - **Athermal defect migration is possible in some materials**

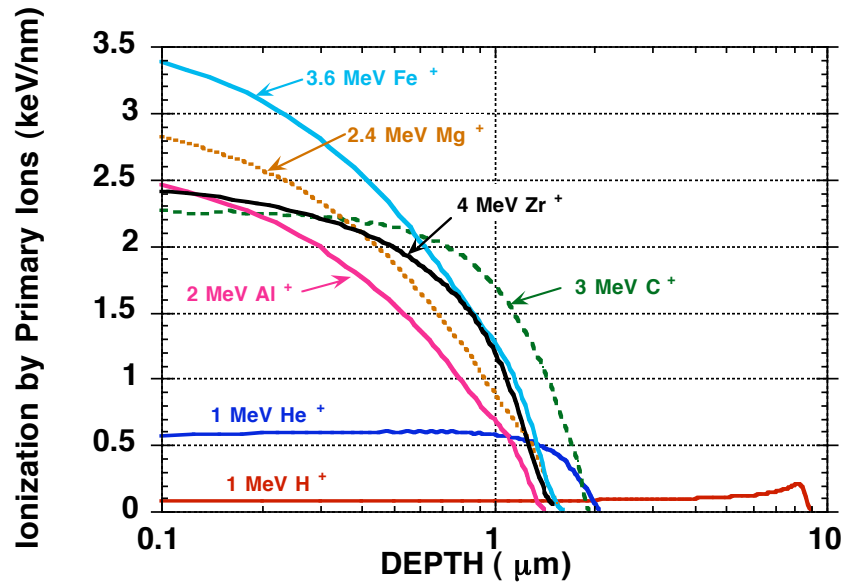
- **Defect production**
 - **Radiolysis (SiO_2 , alkali halides)**
 - **Ion track damage (“swift heavy ions”)**

Conventional ions produce electronic stopping powers up to a few keV/nm in ceramics

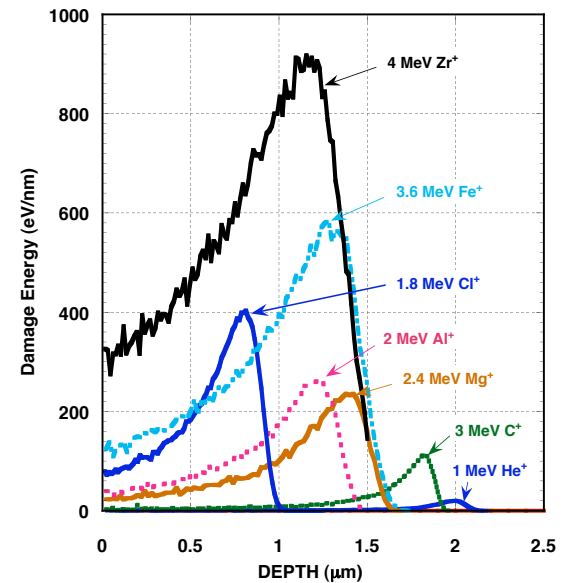
Energy loss is dominated by ionization events

Damage energy = nuclear stopping power minus recoil ionization energy

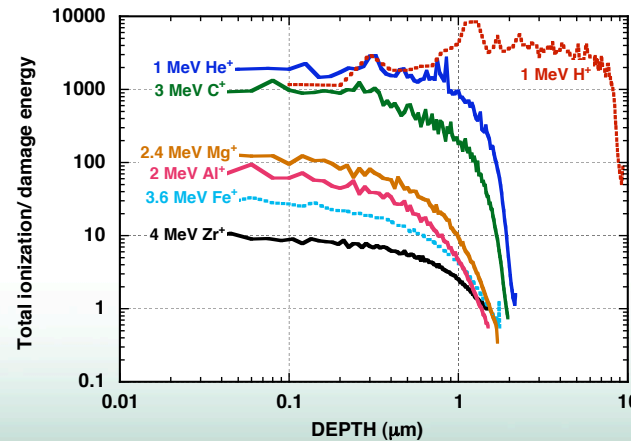
ELECTRONIC STOPPING POWERS IN ALUMINA



DEPTH-DEPENDENT DAMAGE ENERGY IN ALUMINA



RATIO OF TOTAL (ION AND RECOILS) IONIZATION TO THE DAMAGE ENERGY



IONIZATION INDUCED DIFFUSION IN CERAMICS

(cf. Bourgoin & Corbett, Rad. Effects 36 (1978) 157)

- **Energy release mechanism**
 - electron-hole recombination on a defect site provides thermal energy
- **“Normal ionization enhanced diffusion”**
 - an ionized defect charge state may have a lower E_m compared to nonionized defect
- **Bourgoin-Corbett (bistable defect) mechanism**
 - possible iff stable site for ionized state corresponds to the migration saddle point for the non-ionized defect charge state (and vice versa)

Simplified Rate Equations for Ionized Frenkel Defects

(assume only one sublattice, low hole mobility, etc. for simplicity)

$$\frac{dC_v}{dt} = (1 - \epsilon_{ion})P - G_{eh}C_v - \alpha_{i,v}C_v[C_i + C_i^+] - K_s C_v C_s + \alpha_{e,v}^+ C_v^+ n_e + \dots$$

FD production FD ioniz. recombination sinks eln. capture
by beam

$$\frac{dC_v^+}{dt} = (\epsilon_{ion})P + G_{eh}C_v - \alpha_{i,v}^+ C_v^+[C_i + C_i^+] - K_s C_v^+ C_s - \alpha_{e,v}^+ C_v^+ n_e + \dots$$

$$\frac{dC_i}{dt} = (1 - \epsilon_{ion})P - G_{eh}C_i - \alpha_{i,v}C_i[C_v + C_v^+] - K_s C_i C_s + \alpha_{e,i}^+ C_i^+ n_p + \dots$$

$$\frac{dC_i^+}{dt} = (\epsilon_{ion})P + G_{eh}C_i - \alpha_{i,v}^+ C_i^+[C_v + C_v^+] - K_s C_i^+ C_s - \alpha_{e,i}^+ C_i^+ n_p + \dots$$

$$\frac{dn_e}{dt} = G_{eh} - K_1 n_e n_p - K_2 n_e C_v^+ - \dots$$

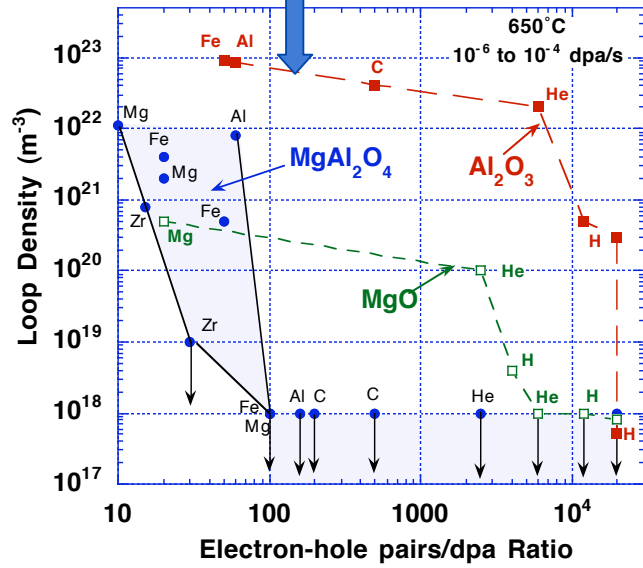
$$\frac{dn_p}{dt} = G_{eh} - K_1 n_e n_p - K_3 n_p C_v - \dots$$

Typical conditions for 1 $\mu\text{A}/\text{cm}^2$ ion beam (~ 1 MGy/s) in insulators: $N_e \sim 10^{-12}/\text{atom}$;
 $G_{eh} \sim 0.01/\text{atom-s}$ \Rightarrow direct ionization by ion beam dominates point defect ionization

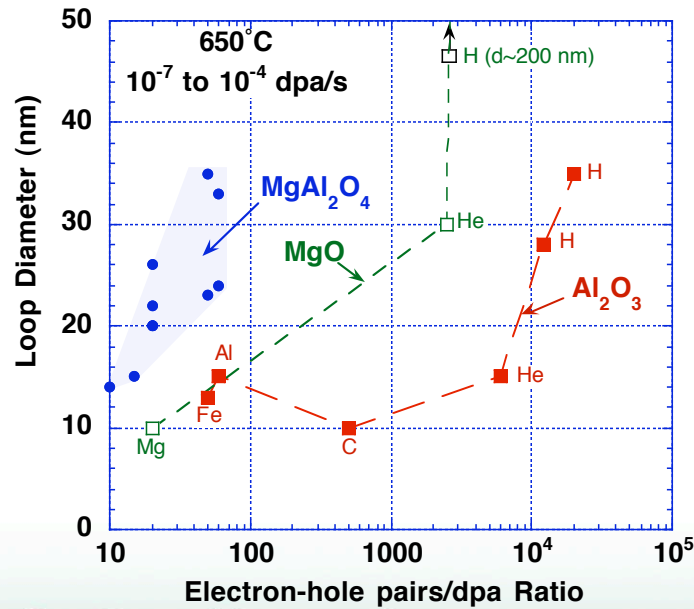
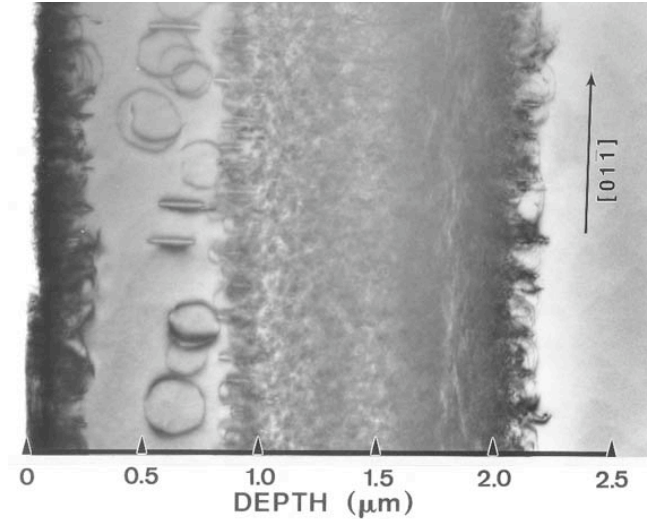
typically $\epsilon_{ion}P \gg G_{eh}C_v \Rightarrow$ uniform ionization in dual ion beam irradiations should have a weak effect on production

Investigation of ionization-induced diffusion in ceramics

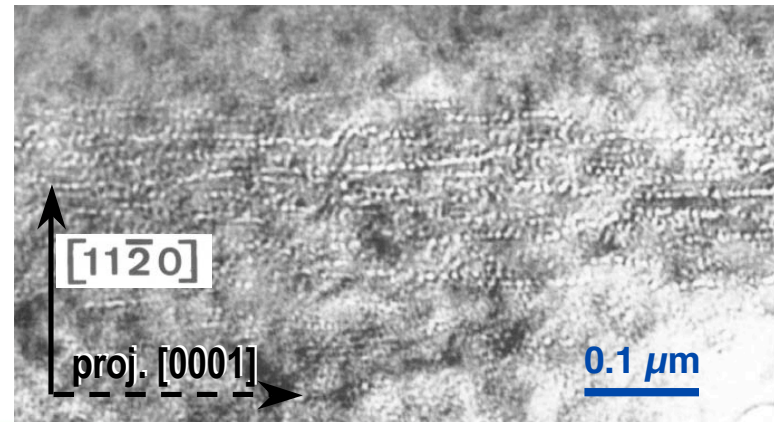
Fission neutron
condition



Large interstitial loops in MgAl_2O_4 ion-irradiated at 25°C for regions with >100 eln.-hole pairs per dpa

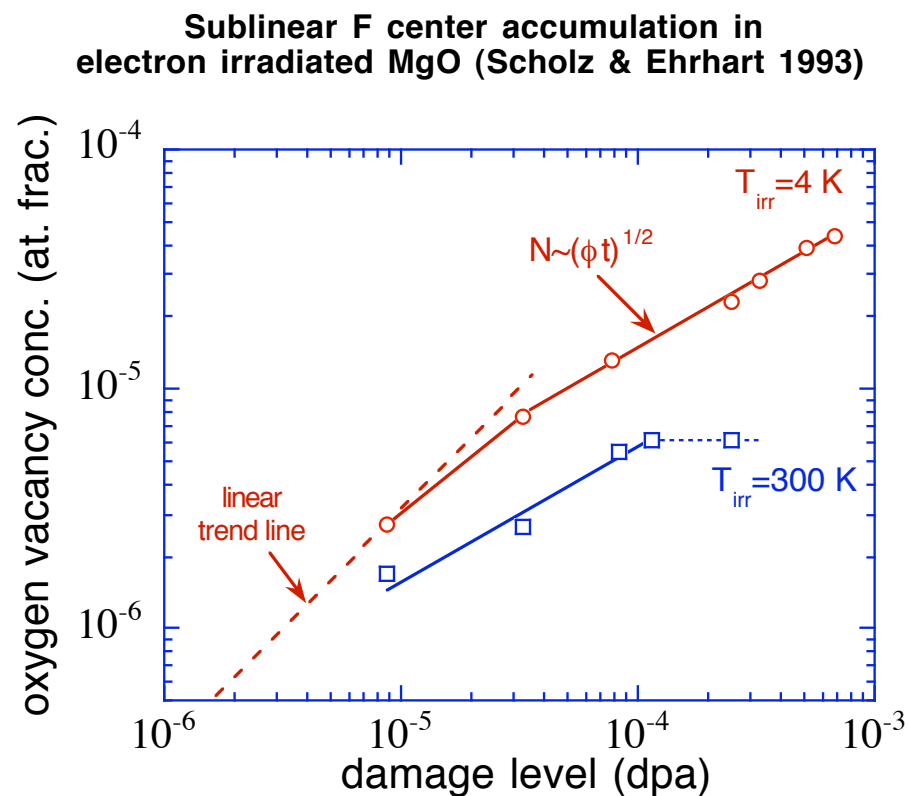
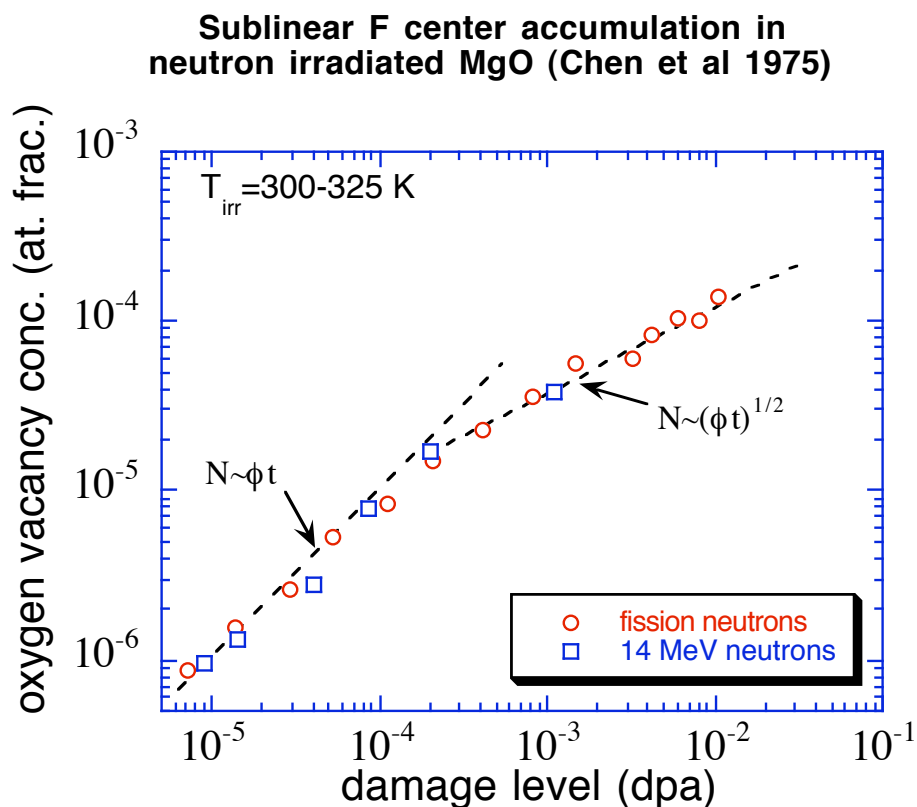


Aligned cavities in Al_2O_3 ion-irradiated at 25°C (Al/O/He ion irradiation, >500 eln.-hole pairs per dpa)



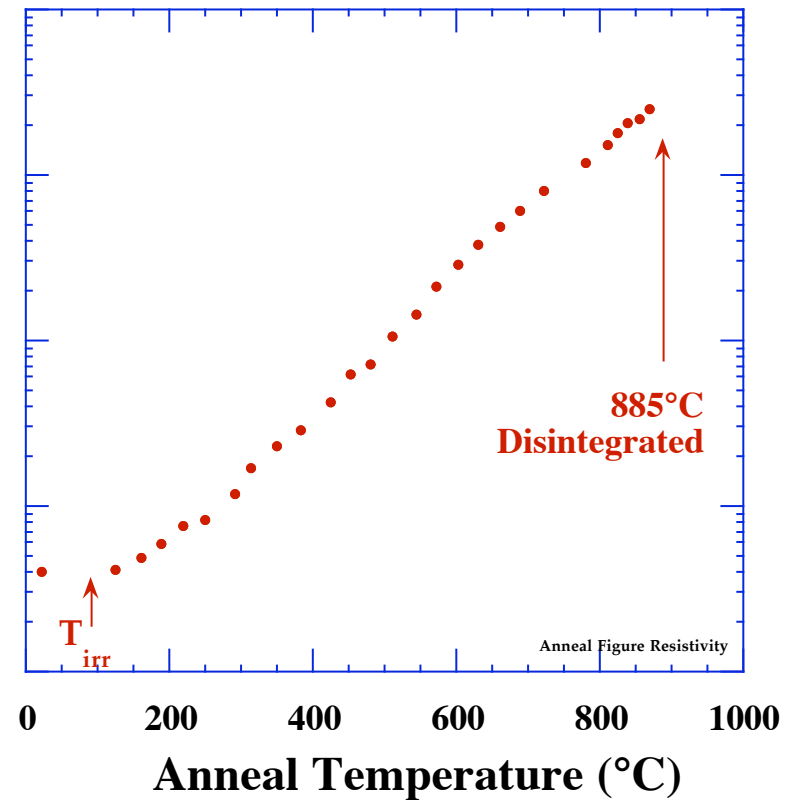
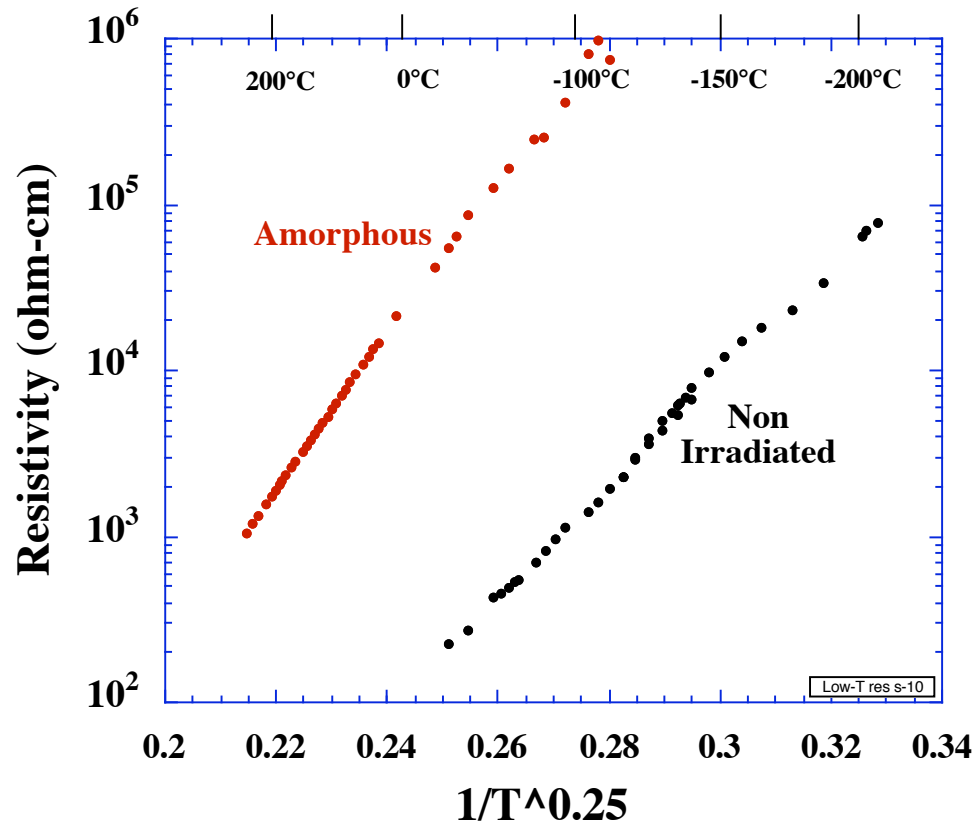
Square root fluence dependence of defect accumulation is an indication of uncorrelated point defect recombination

- Ionizing radiation may induce athermal point defect recombination in some ceramics



Physical Properties Below Crystallization Temperature

- Amorphized Morton CVD SiC -

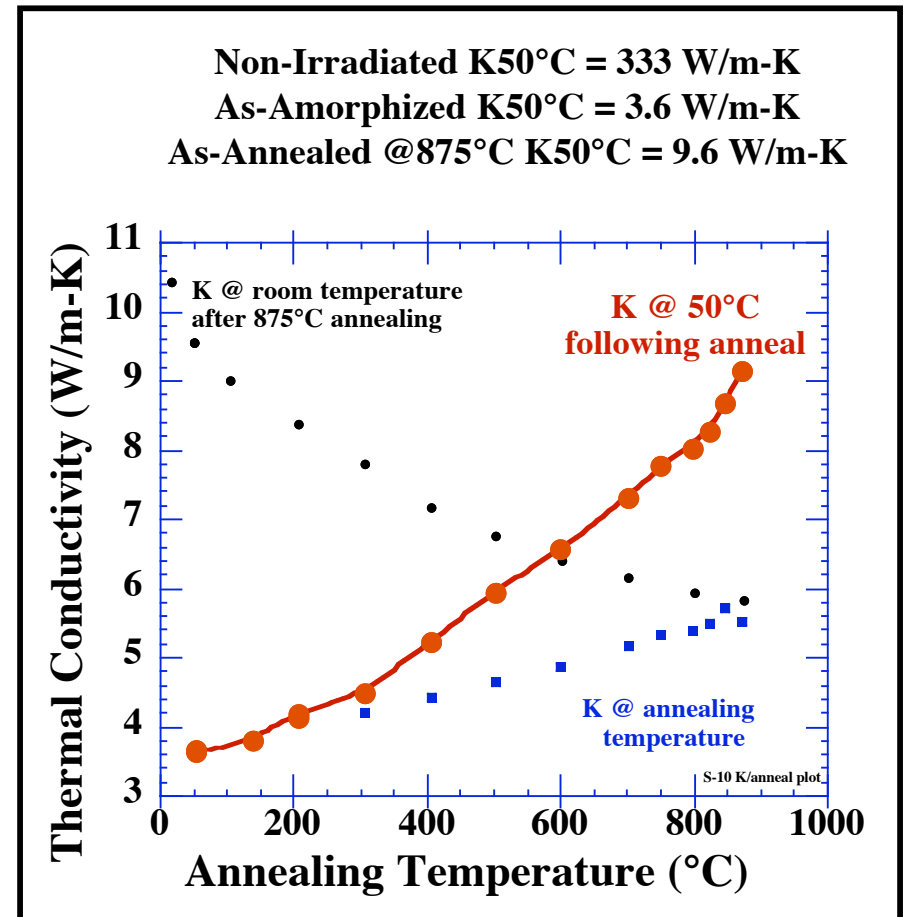
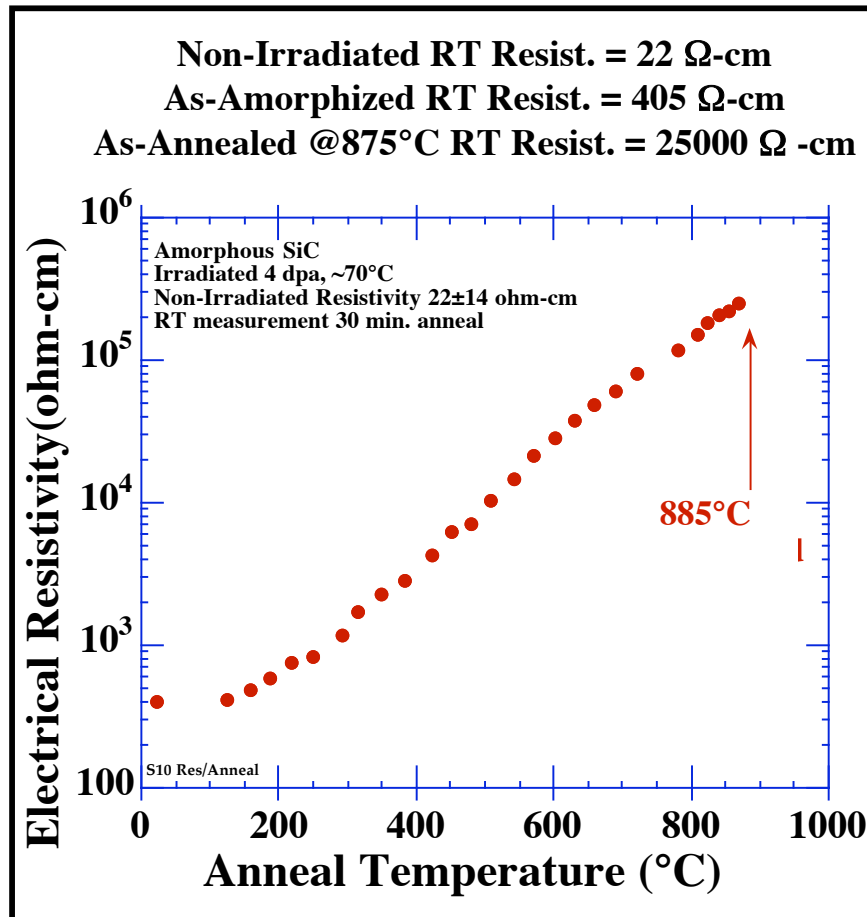


- Temperature dependence follows $T^{-1/4}$ dependence indicating hopping conduction.
- Reducing the density of states increases the conductivity up to the point of crystallization.

Snead & Zinkle, Nucl. Instr. Meth. B 191 (2002) 497

Physical Properties of amorph. SiC Below Recrystallization Temperature

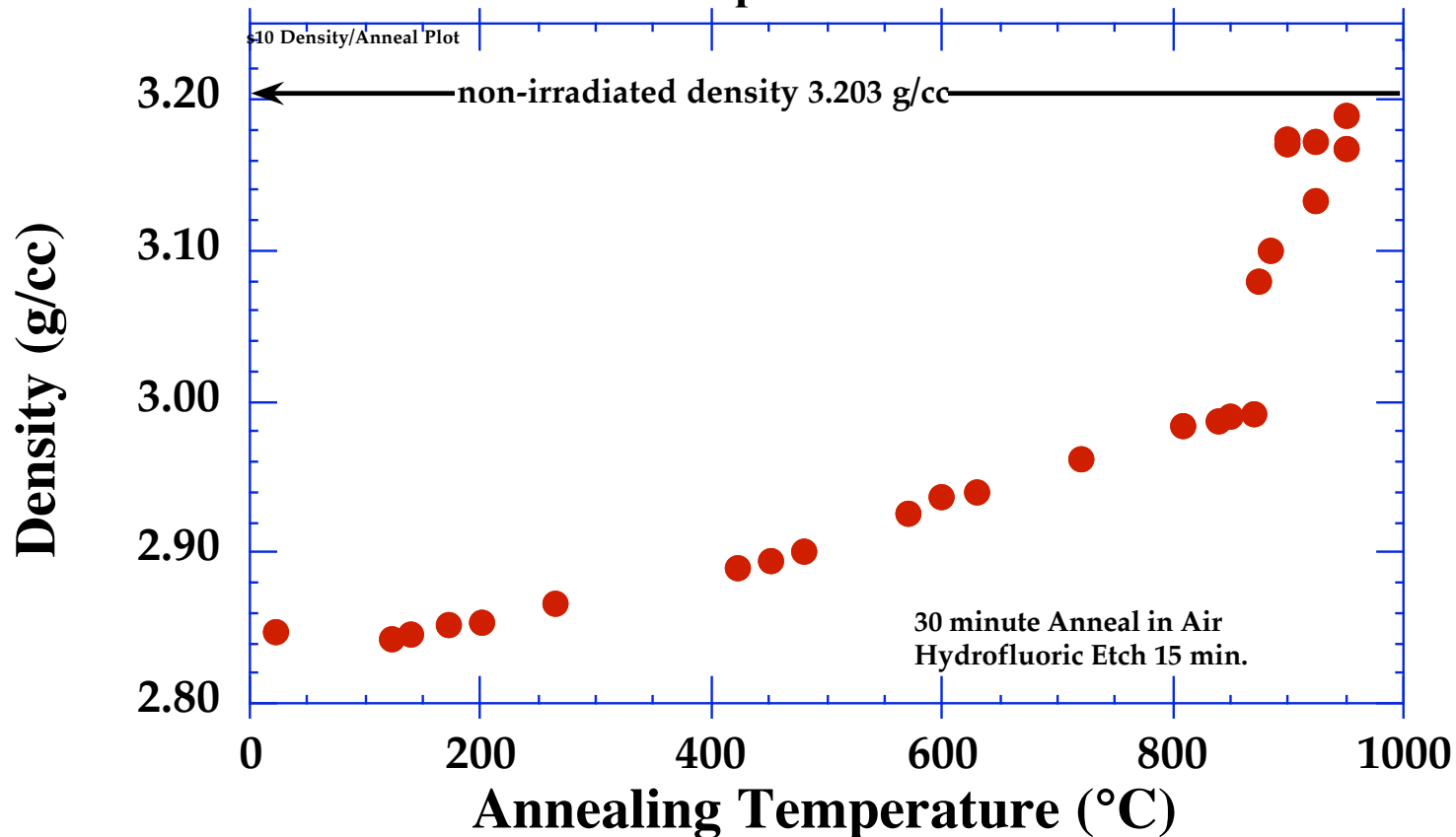
Continual variation in the properties of amorphous SiC occurs prior to recrystallization
Numerous short-range ordered configurations can exist in amorphous material



- Local strain is reduced upon annealing, leading to lower phonon scattering

Physical Properties Below Crystallization Temperature

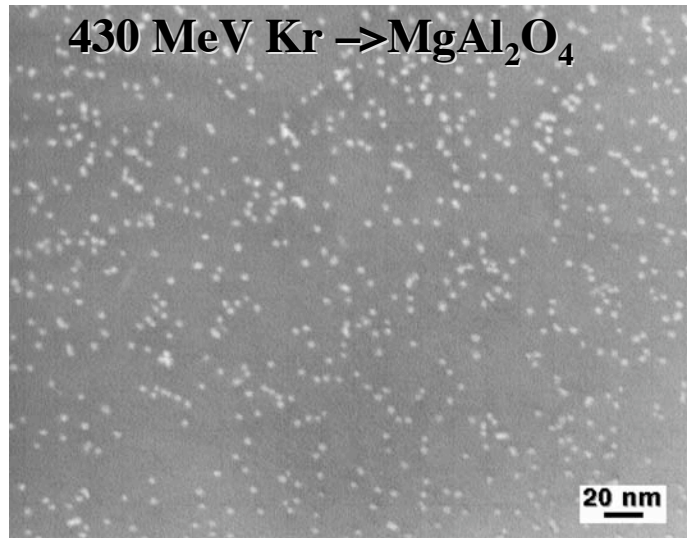
Amorphous SiC



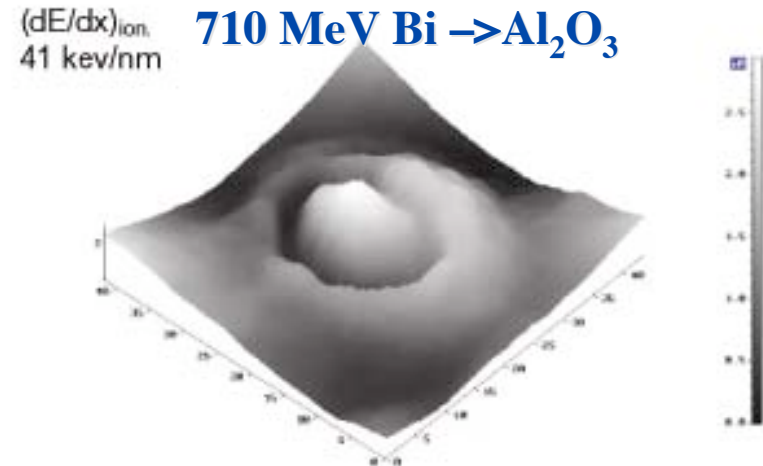
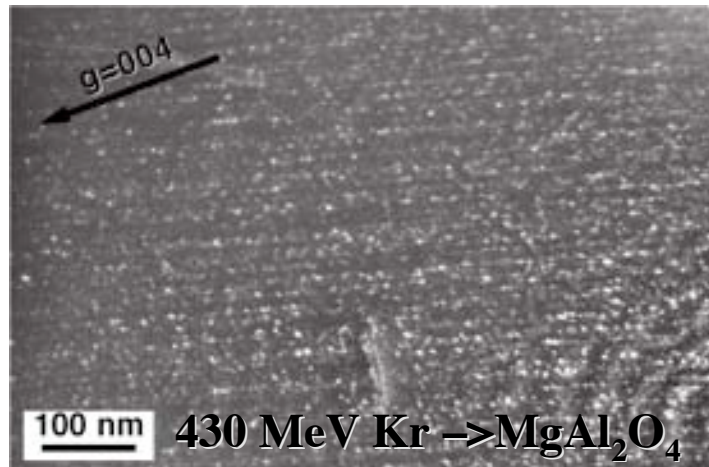
- Amorphous structural relaxation occurs from irradiation temperature to $\sim 875^{\circ}\text{C}$ yielding $\sim 4.8\%$ increase in density.
- Explosive crystallization occurs at $875\text{-}885^{\circ}\text{C}$, reaching near theoretical density by 950°C .

Snead & Zinkle, Nucl. Instr. Meth. B 191 (2002) 497

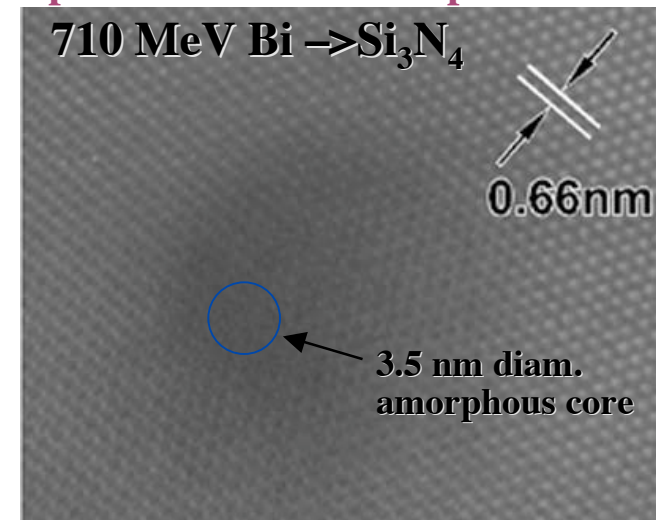
Highly ionizing radiation ($dE_{\text{ioniz.}}/dx > 7 \text{ keV/nm}$) introduces new damage production mechanisms



Ion tracks produce displacement damage via inelastic atomic events



Swift heavy ions induce surface protrusions and amorphization



Overview of radiation damage parameters of importance in irradiated semiconductors and insulators

- **deposited energy: Grays**
 - (1 Gy=100 rads; typical chest X-ray ~1mGy)
- **lattice damage: displacements per atom (dpa)**
 - (complicated for ceramics due to multiple sublattices and ion masses)
- **gaseous transmutations (H, He)**
 - 14 MeV neutrons: ~100 appm/dpa
 - fission neutrons: ~ 1 appm/dpa

- **Insulators, Semiconductors and Metals (electron energy bands)**
 - insulator: $\rho_e > 10^4 \Omega\text{-m}$ (typical joule heating limit)
- **Ionizing Radiation Causes Increase in Electrical Conductivity**
 - prompt effects (radiation induced conductivity)
 - permanent effects (radiation induced electrical degradation)
- **Measurements Must be Made In-Situ**
 - RIC recovers quickly (typically prompt lifetime \sim ns)
 - RIED requires an applied electric field while displacement damage is occurring
- **Impact of RIC and RIED**
 - possible decalibration of diagnostics or failure of ceramic insulators in nuclear or accelerator systems

- **NECESSARY CONDITIONS FOR RIED**

- **1) Ionizing radiation (RIC)**

- **2) Displacement damage**

- **3) Applied electric field ($E > 100$ V/mm)**

- **4) Intermediate irradiation temperature (300-600°C)**

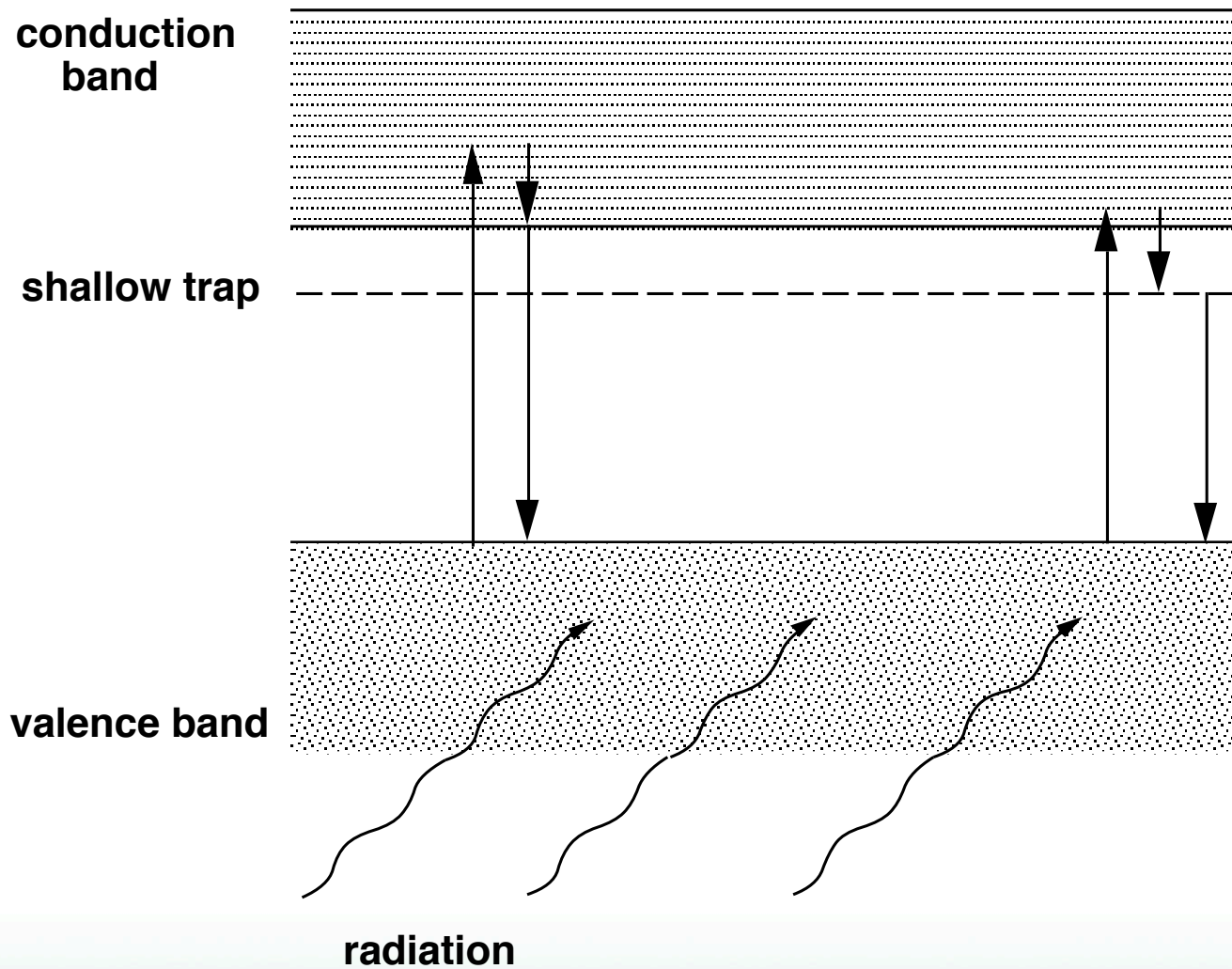
- **PHYSICAL MECHANISM ????**

- **1) Localized thermoelectric breakdown**

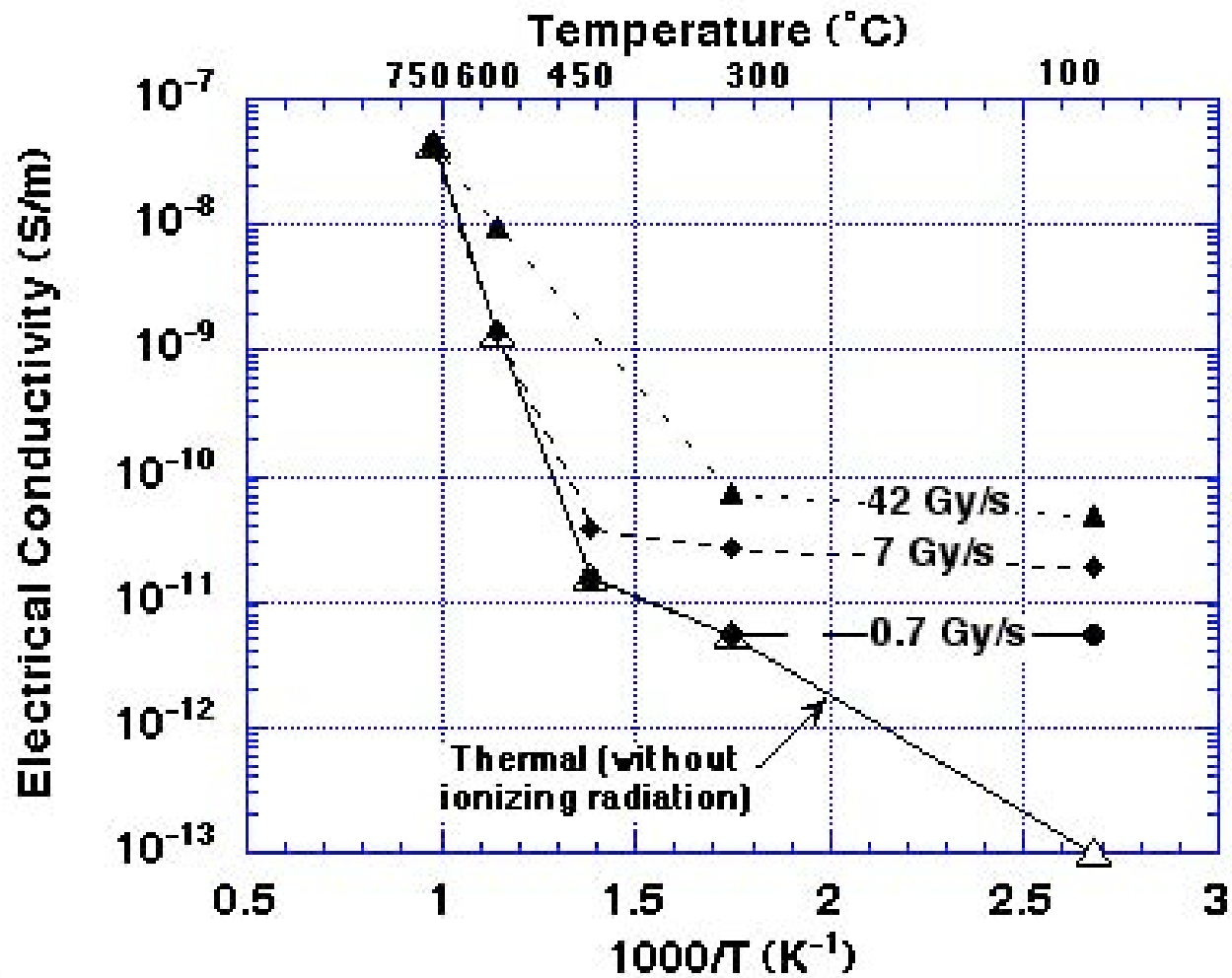
- **2) Colloid formation**

- **3) Experimental artifact (surface contamination / microcracking)**

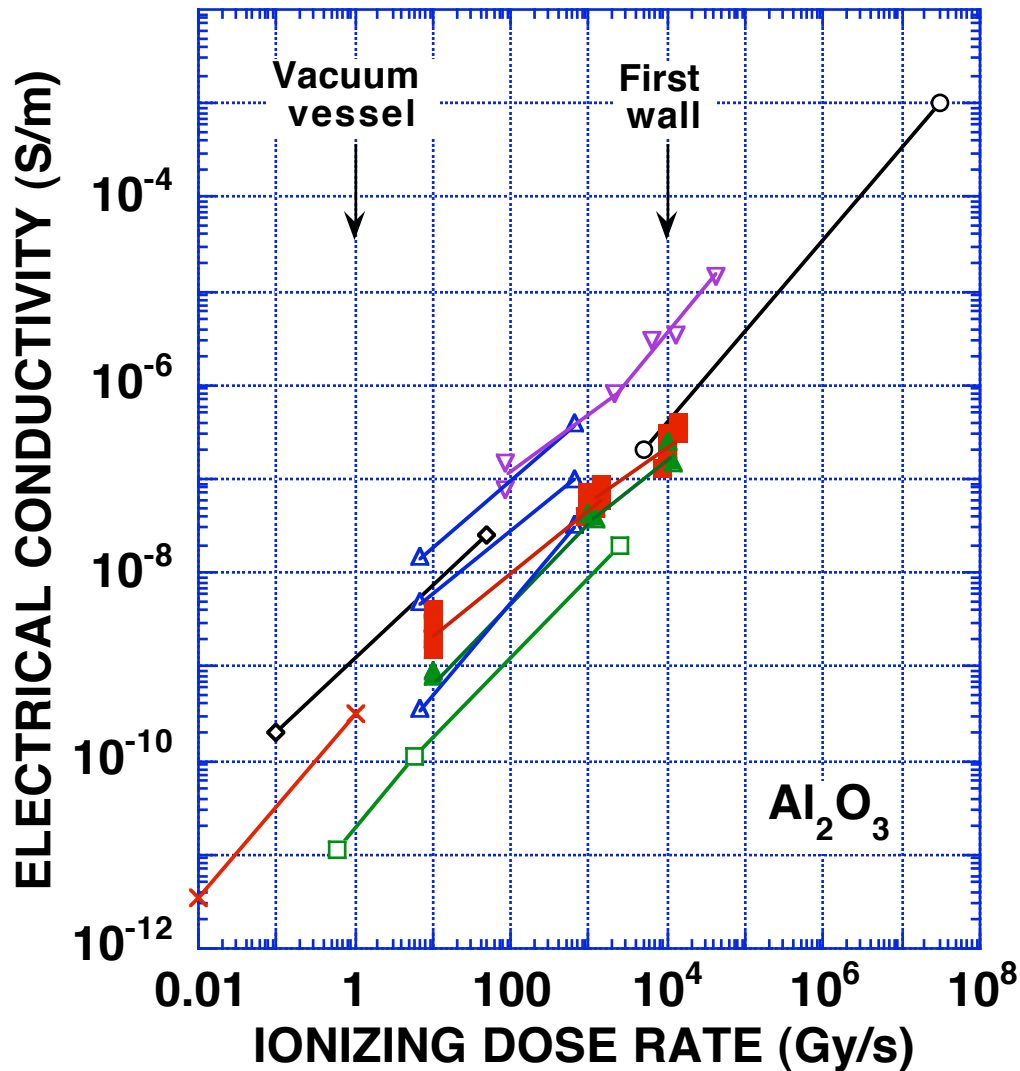
Radiation Induced Conductivity in Insulators



Electrical conductivity components in fine-grained 99.99% purity alumina cable ("CR125")



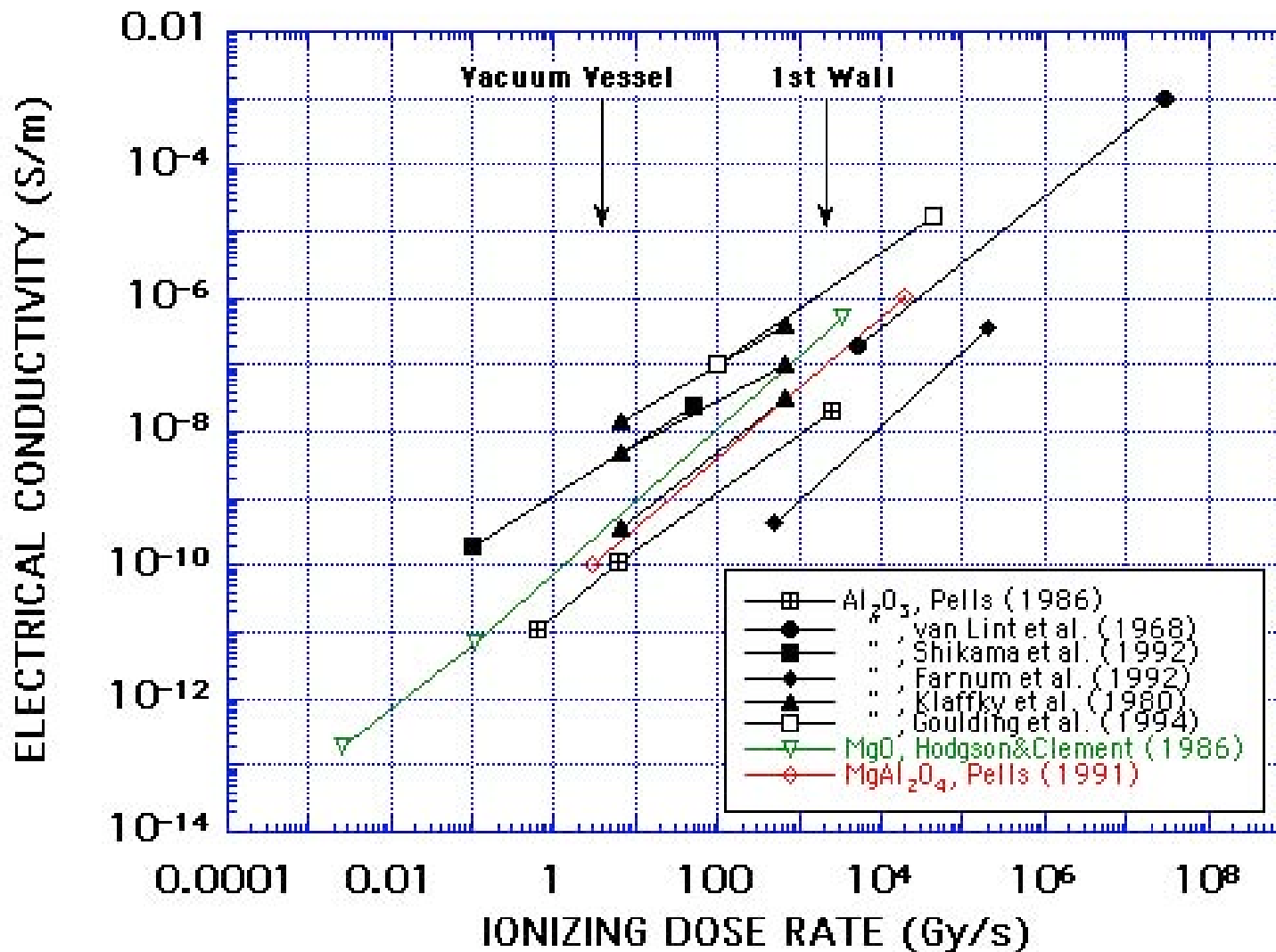
Summary of RIC results for Al_2O_3



- RIC is proportional to ionizing radiation flux
 - Similar results obtained for X-ray, electron, ion and neutron irradiation
- Proportional constant for RIC depends on impurities in ceramic (electron trapping)
 - Lowest RIC occurs in ceramics with highest impurity concentration

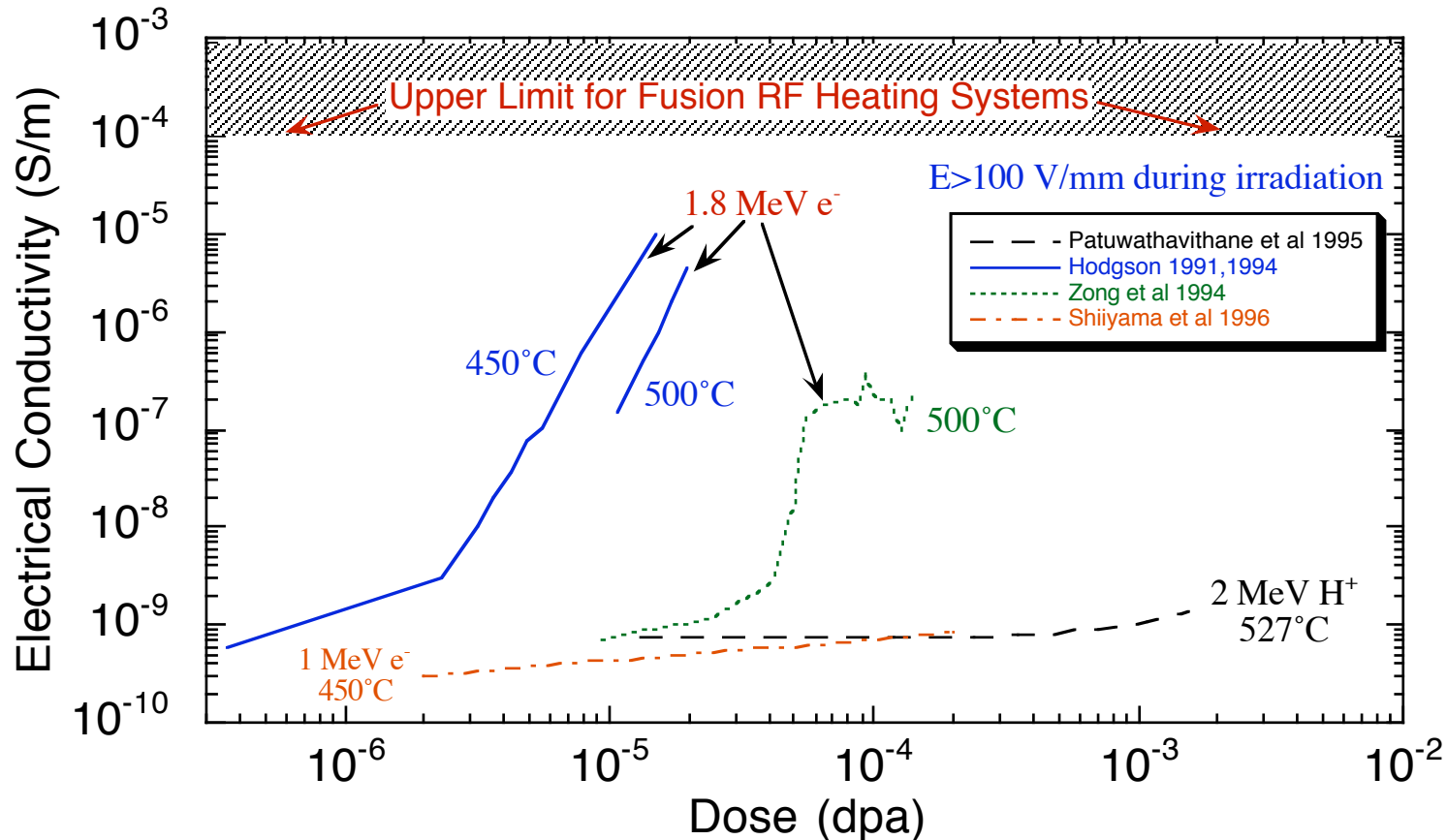
RIC behavior is qualitatively similar in all wide band gap ceramic insulators

RADIATION INDUCED CONDUCTIVITY IN OXIDE CERAMICS



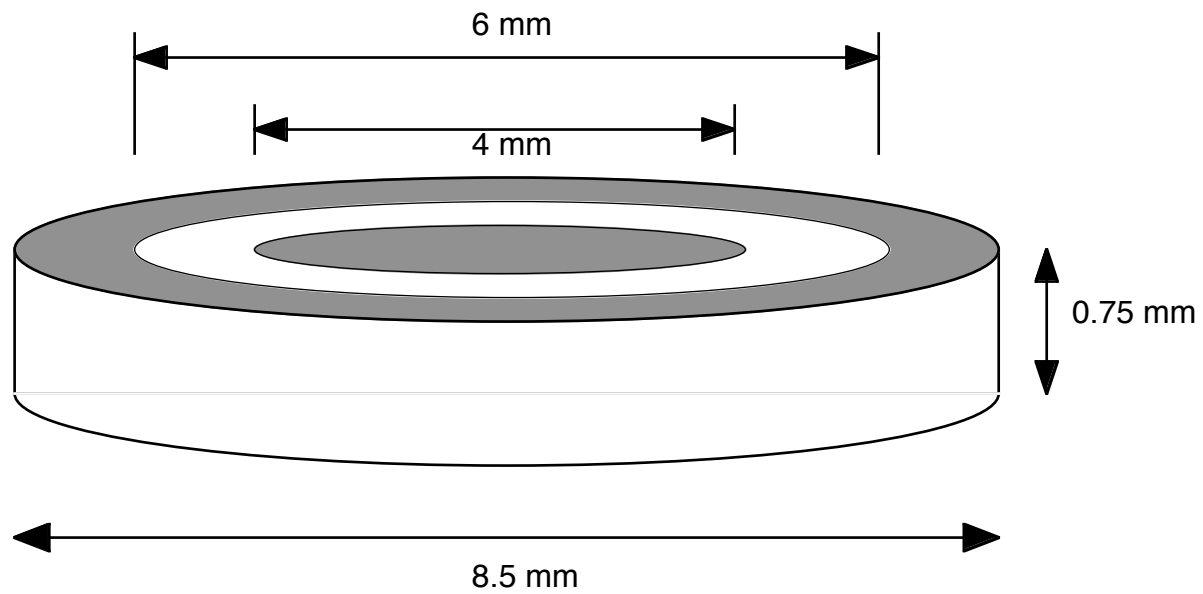
The “Radiation-Induced Electrical Degradation” Controversy

RIED studies on single crystal alumina at 450-530°C

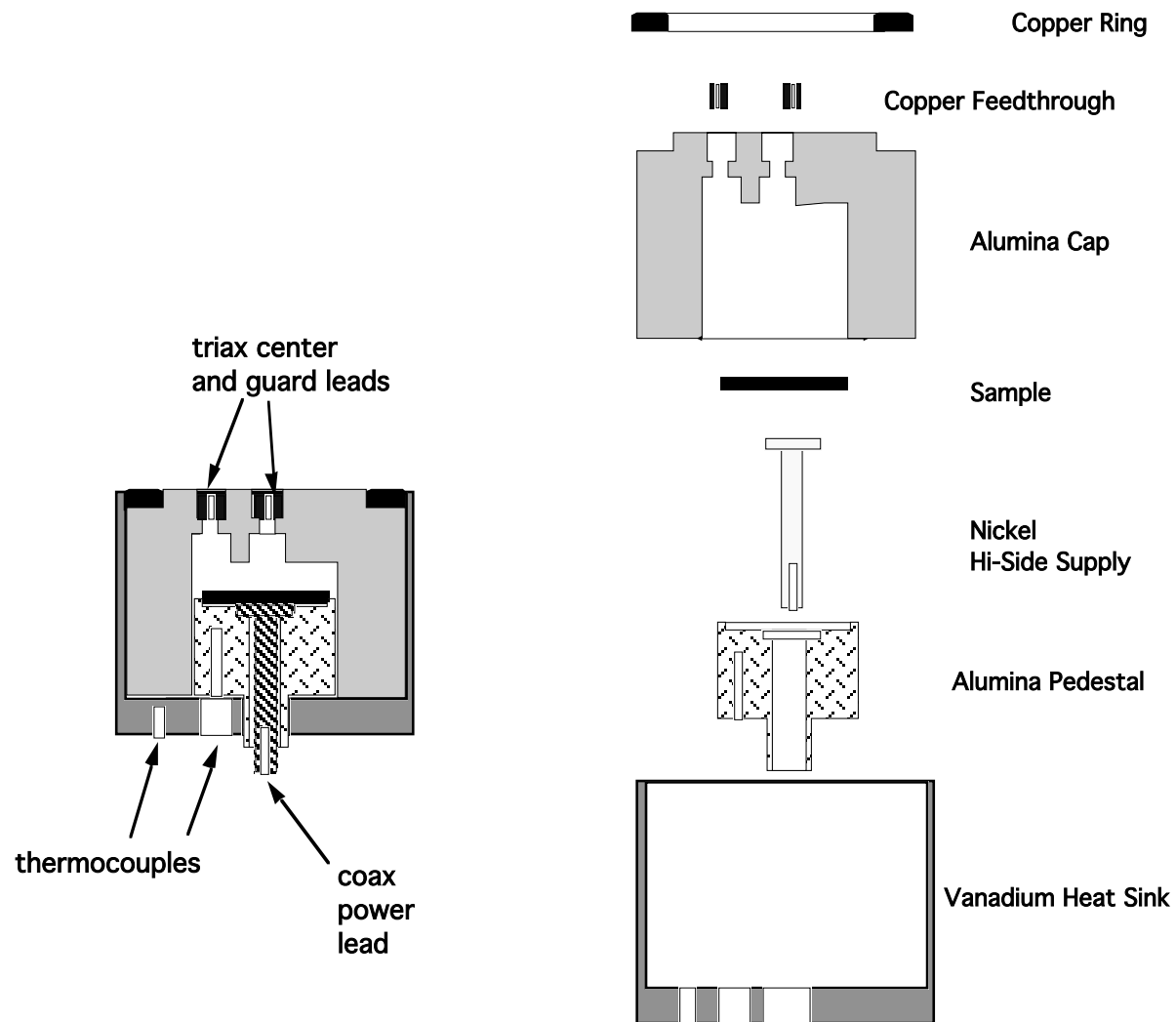


- Observed in several electron irradiation studies
 - Mechanism associated with formation of metallic colloids?

GUARDED ELECTRODE GEOMETRY FOR HFIR ELECTRICAL RESISTIVITY EXPERIMENTS ON CERAMIC INSULATORS

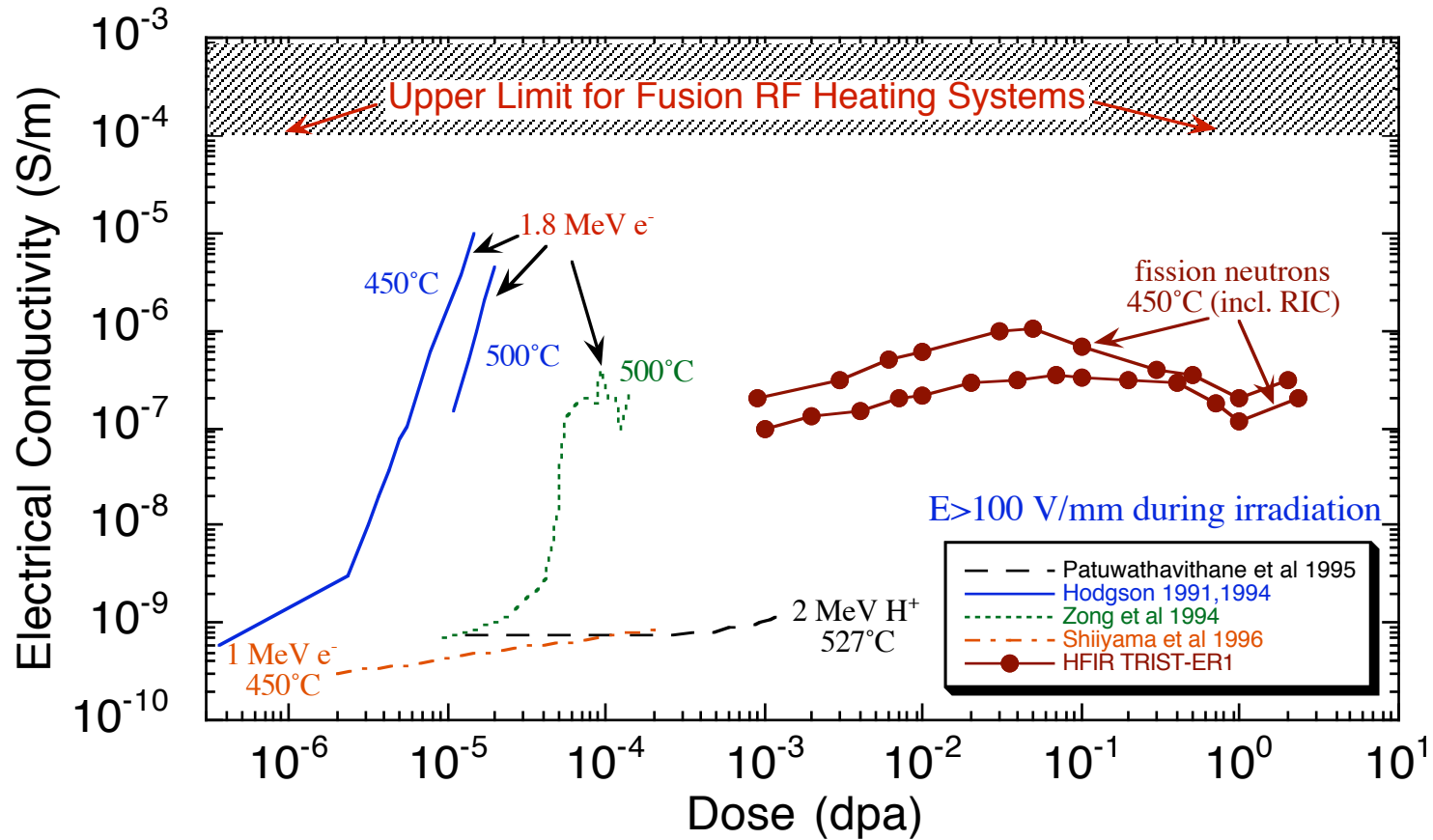


Schematic of fission reactor irradiation capsule for in-situ electrical conductivity measurements



The phenomenon of Radiation Induced Electrical Degradation does not appear to be of concern for ITER

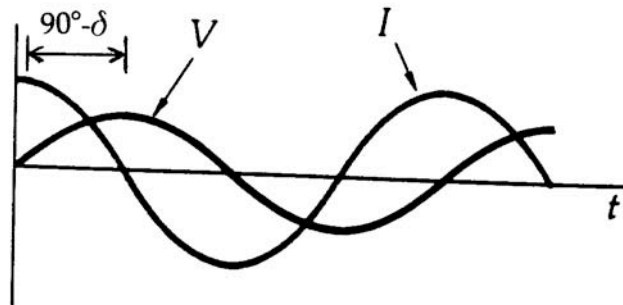
RIED studies on single crystal alumina at 450-530°C



- Several recent high-dose fission reactor studies have not observed RIED

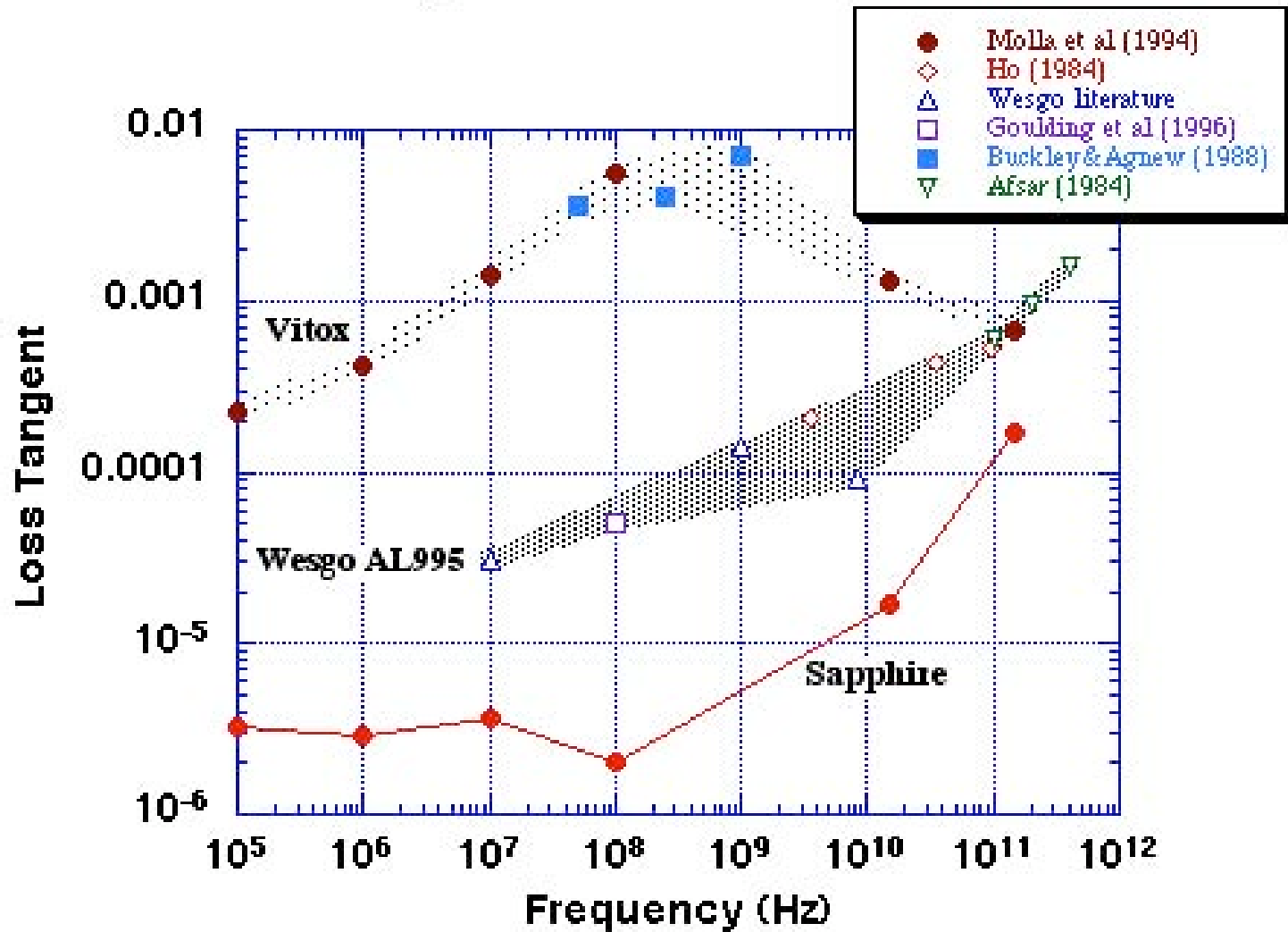
Effect of irradiation on loss tangent

- Power dissipation in dielectrics is proportional to the loss tangent

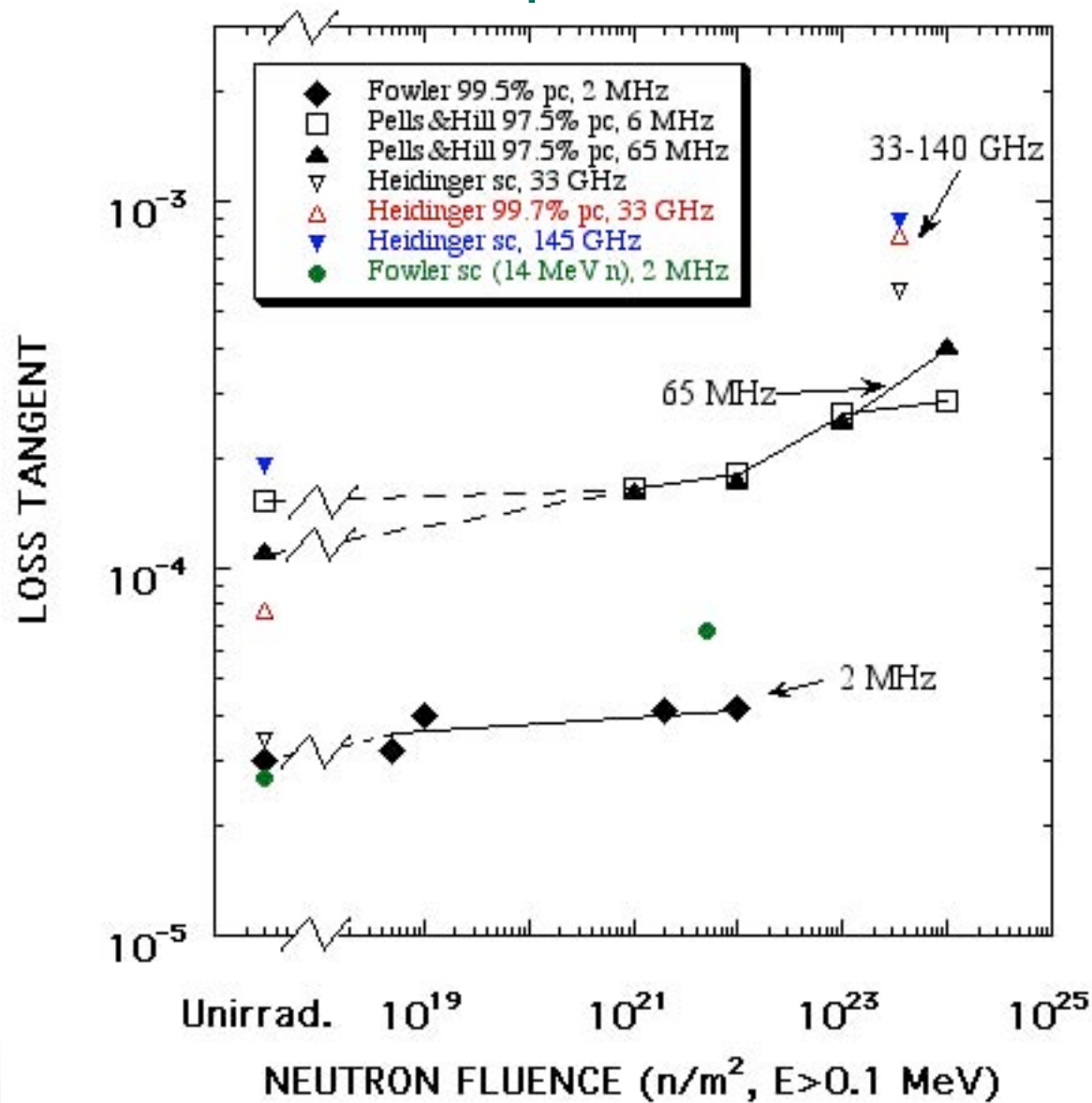


Plots of current I and voltage V across the capacitor versus time. The voltage lags the current by 90° .

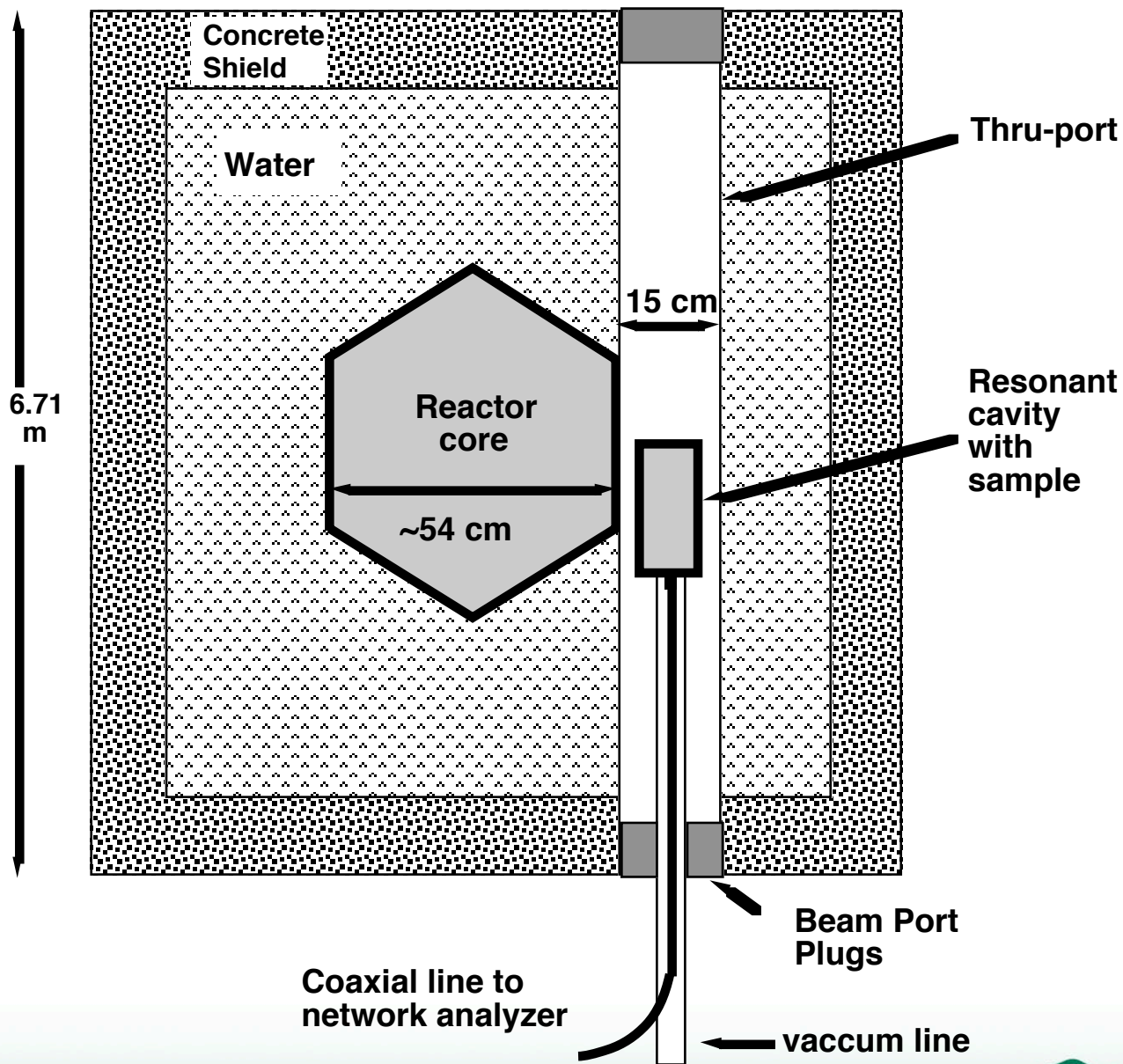
Measured Loss Tangents for Different Grades of Alumina



Loss Tangent in Al₂O₃ Irradiated Near Room Temperature

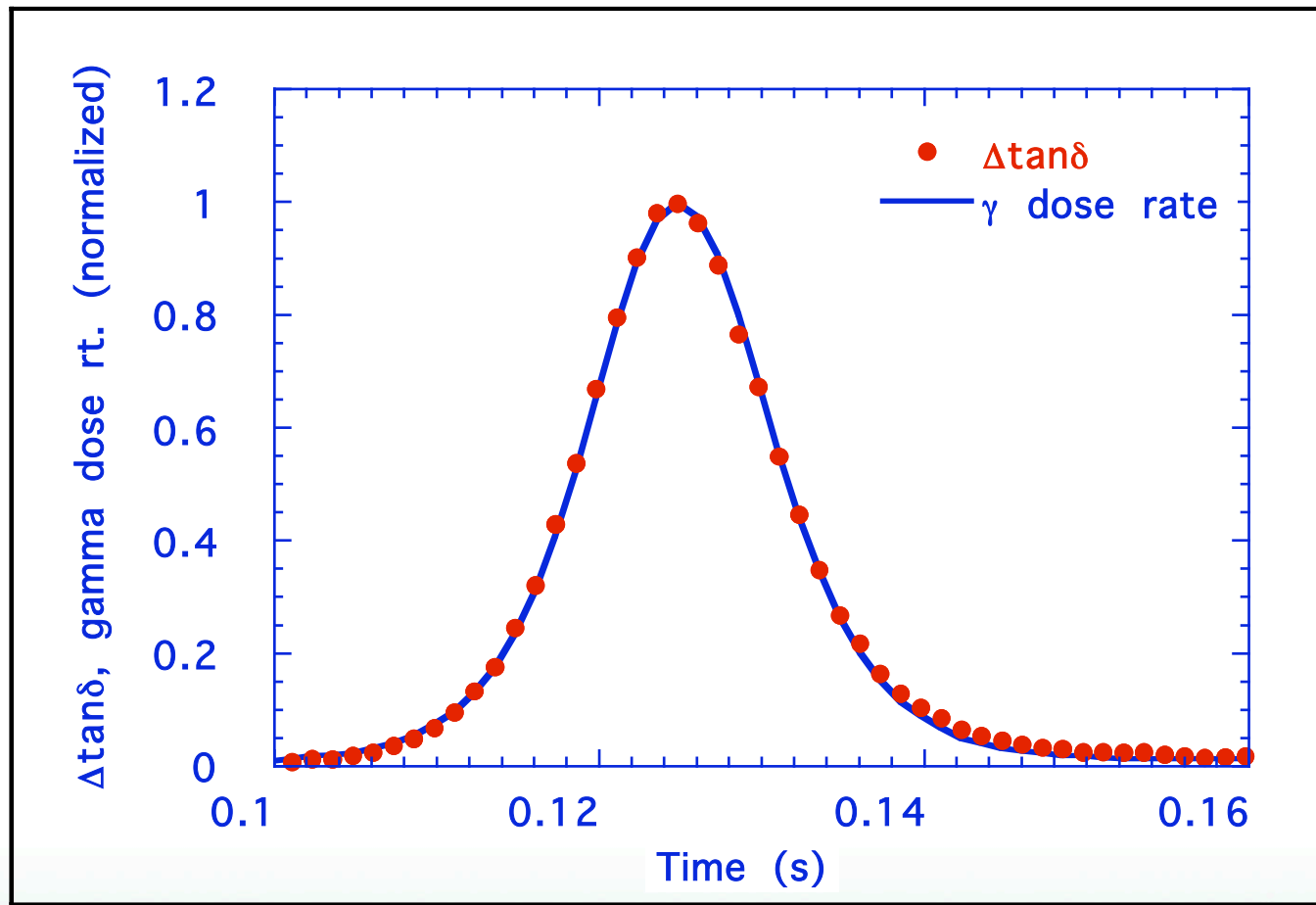


University of Illinois TRIGA Reactor Facility



For most materials tested increase in loss tangent is proportional to the ionizing dose rate

- Example shows overlaid profiles of $\Delta \tan \delta$ and ionizing dose rate for Al998 (both normalized to 1)
- Indicates $\tau_{\text{trapping}} \ll$ pulse rise and fall times



Analysis of Results

- Measured in-situ Al_2O_3 loss tangent results are consistent with published radiation induced conductivity data assuming increased $\tan\delta$ is due to increased σ_{DC} , where

$$\tan\delta = \frac{\sigma_{DC}}{\omega\epsilon'} + \frac{\chi}{\epsilon'/\epsilon_0}$$

- Neutron displacement damage effects are insignificant due to low accumulated damage in the reactor pulse ($<10^{-8}$ dpa)

$$\Delta \tan\delta)_{dpa} = \frac{n(Zea)^2(\epsilon'_\infty + 2)^2}{18\epsilon_0 kT\epsilon'_\infty} < 10^{-5}$$

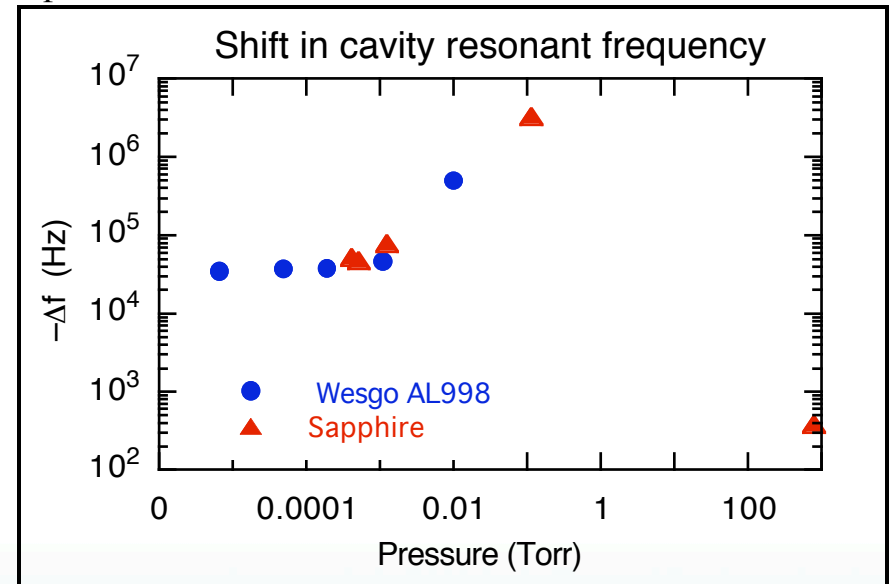
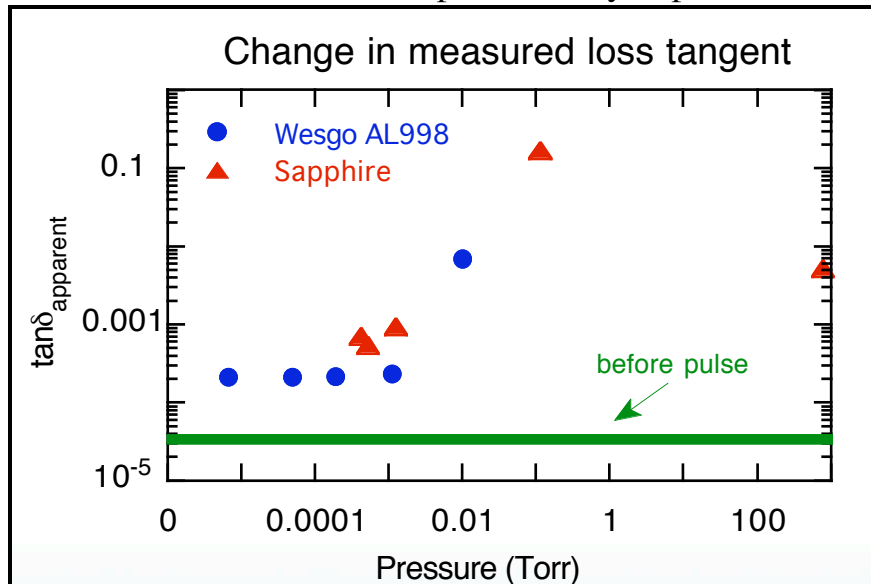
Pressure effects

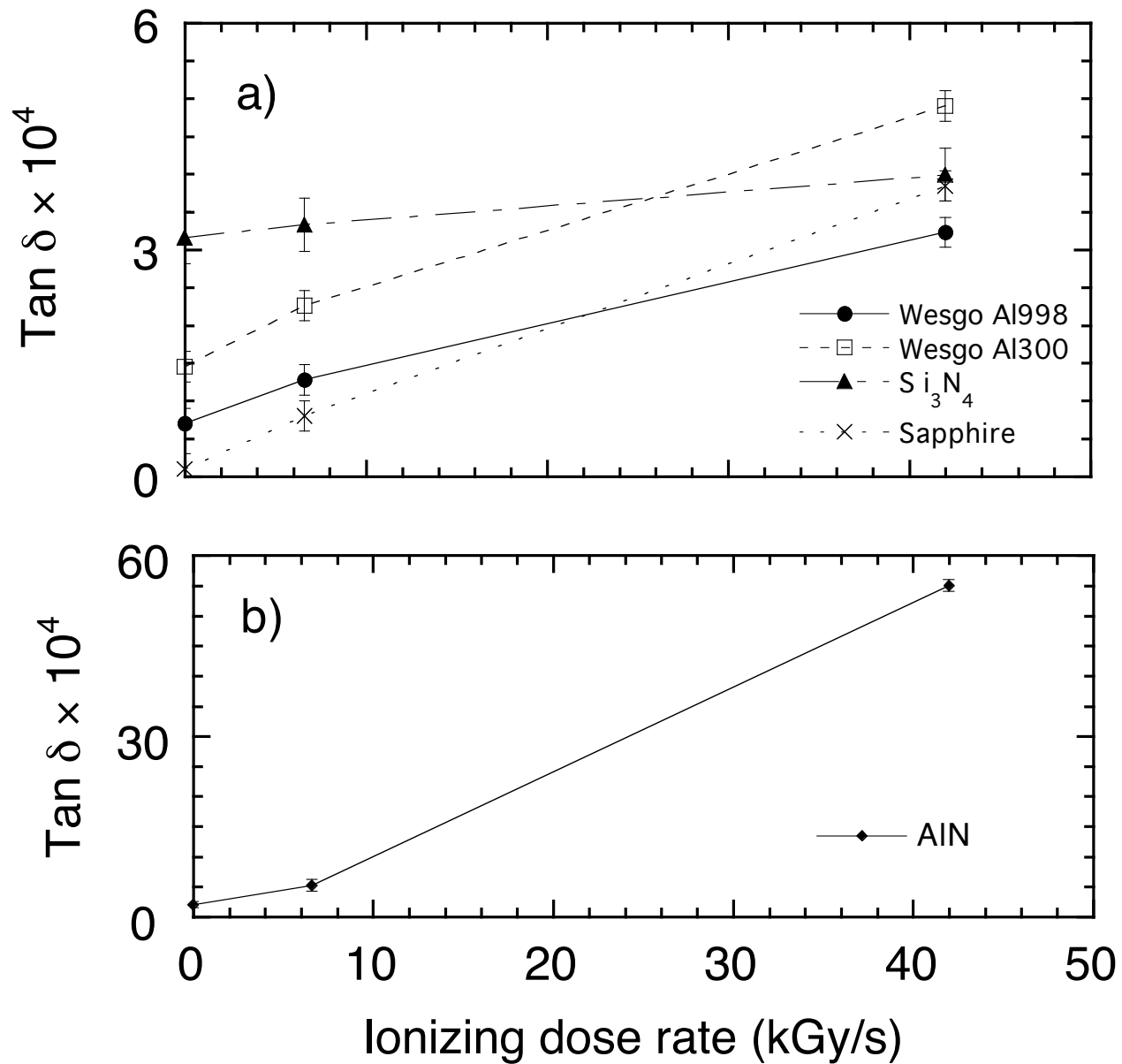
- Gamma flux ionizes residual gas in the cavity,
- Causes spurious losses and frequency shifts which cannot be distinguished from changes in the dielectric properties of the ceramic
- Consistent with a model of the ionized gas as a dielectric with permittivity

$$\epsilon = \epsilon_0 - \frac{n_e e^2}{m(\nu^2 + \omega^2)} - j \frac{n_e e^2 \nu}{\omega m(\nu^2 + \omega^2)}$$

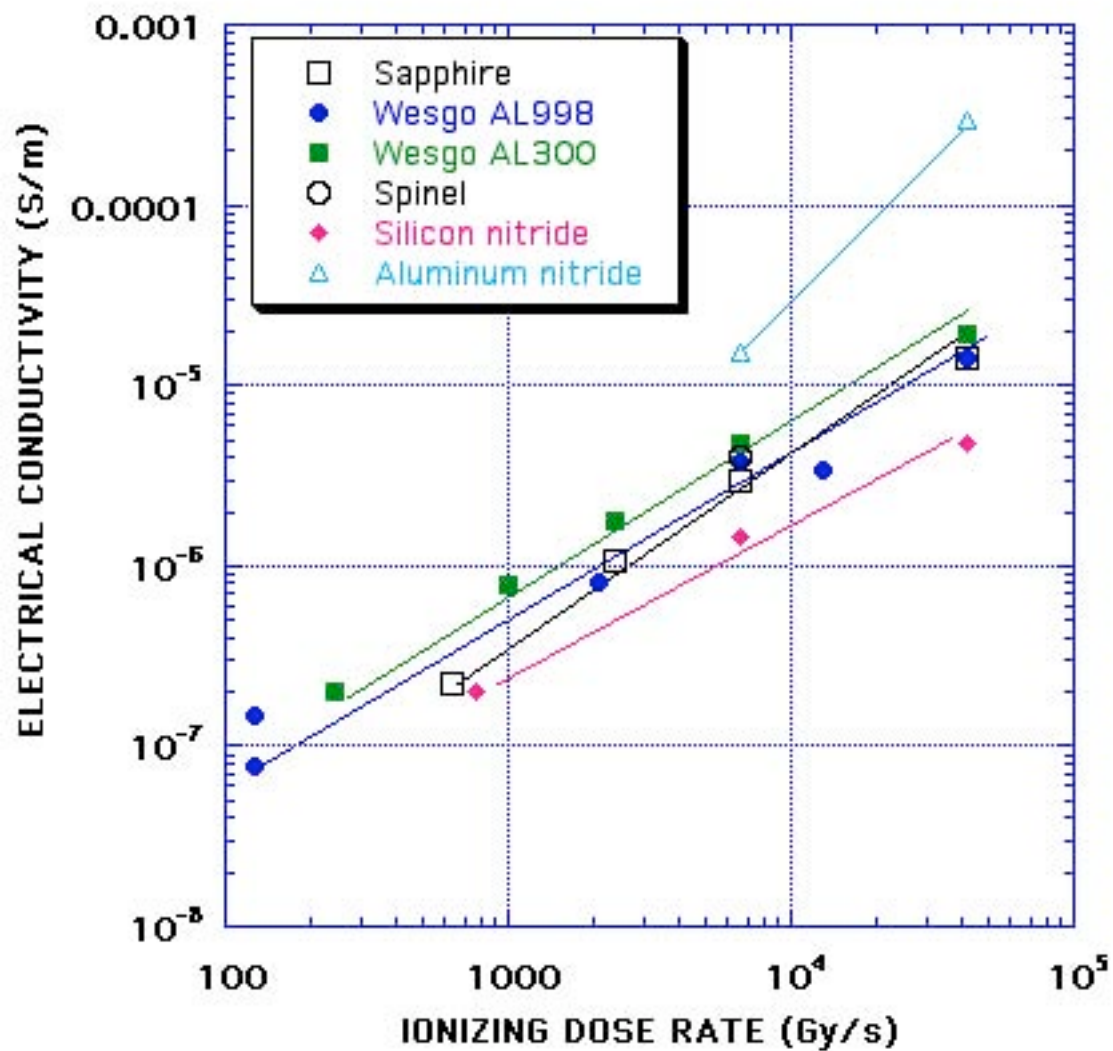
n_e = electron density, ω = applied frequency, ν = collision frequency

- Maximum effect seen experimentally at $p \sim 0.1$ torr, little effect for $p \leq 10^{-4}$ torr

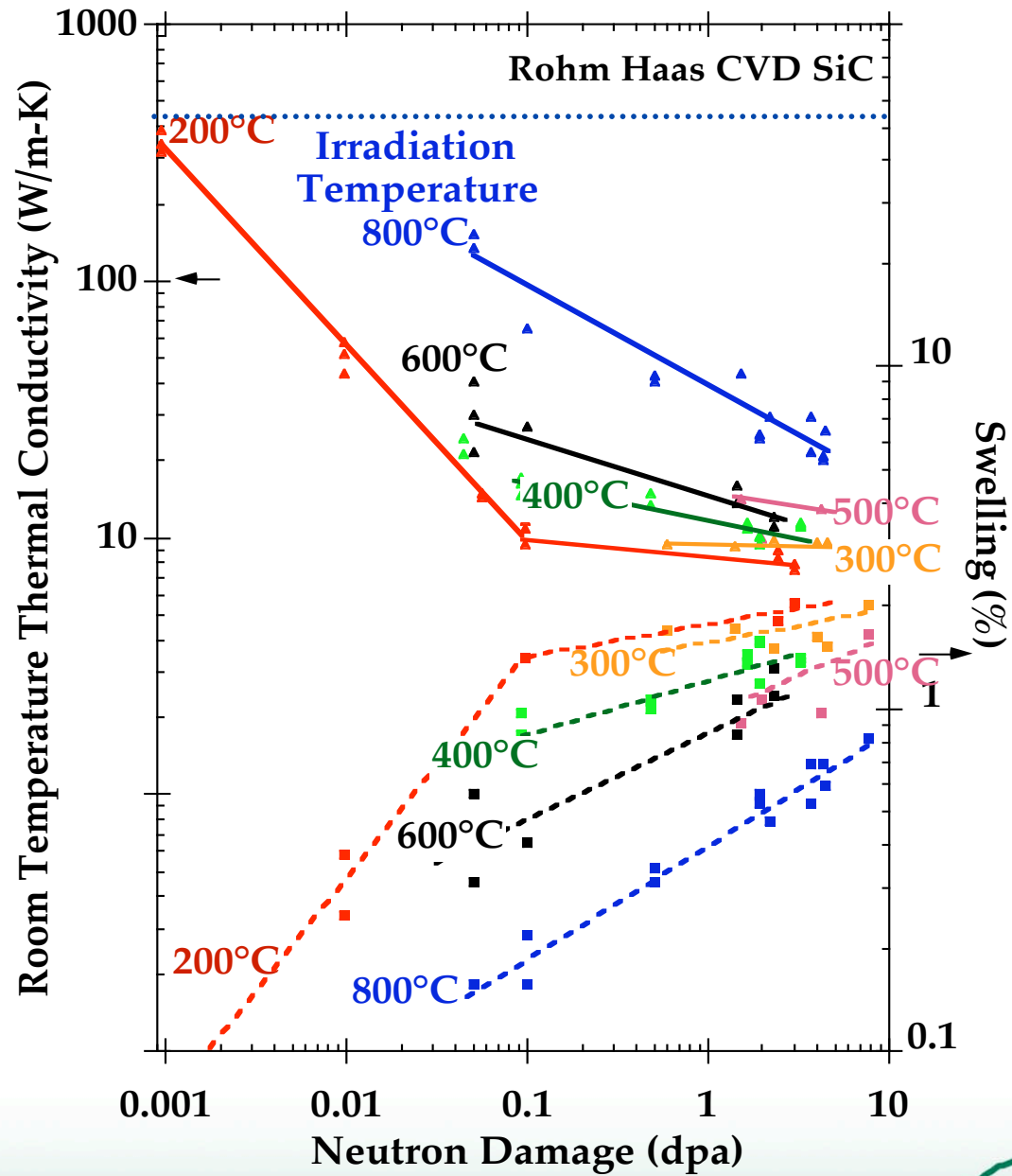




ELECTRICAL CONDUCTIVITY OF CERAMICS DERIVED FROM LOSS TANGENT MEASUREMENTS



Example of Degradation of Thermal Conductivity with Irradiation



Adopting Thermal Defect Resistance

$$[K(T)]^{-1} = \left[\frac{1}{K_u(T)} + \frac{1}{K_{gb}(T)} + \frac{1}{K_{d0}} + \frac{1}{K_{rd}} \right]$$

↓ umklapp
 ↓ boundaries
 ↓ intrinsic defects
 ↓ radiation defects

$$\frac{1}{K_{rd}} = \frac{1}{K_{irr}} - \frac{1}{K_{unirr}}$$

Thermal defect resistance

$$\frac{1}{K_{rd}} = \left(\frac{3\pi}{2k_B} \right) \left(\frac{\Omega \omega_D}{v^2} \right) C_v$$

Thermal defect resistance due to low vacancy production

The main motivation for using thermal defect resistance is that radiation-induced defects, such as vacancies and clusters, have resistances proportional (or square root dependent) to their concentration and are additive. This gives an easy way to compare stability of ceramics under irradiation.

Adopting Thermal Defect Resistance

Thermal defect resistance

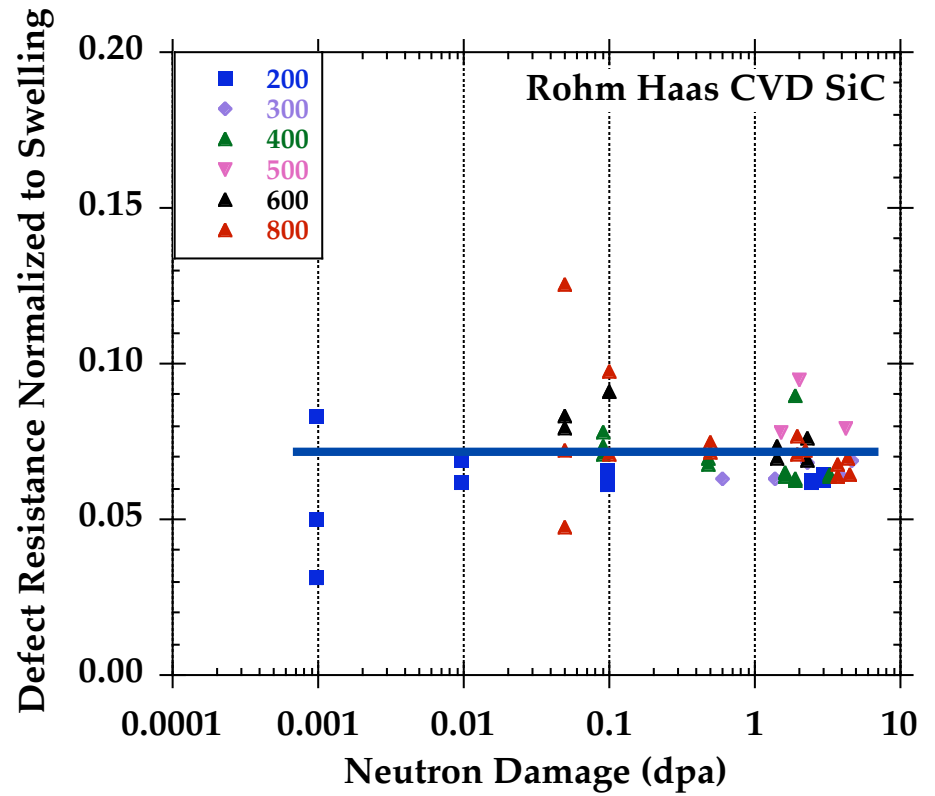
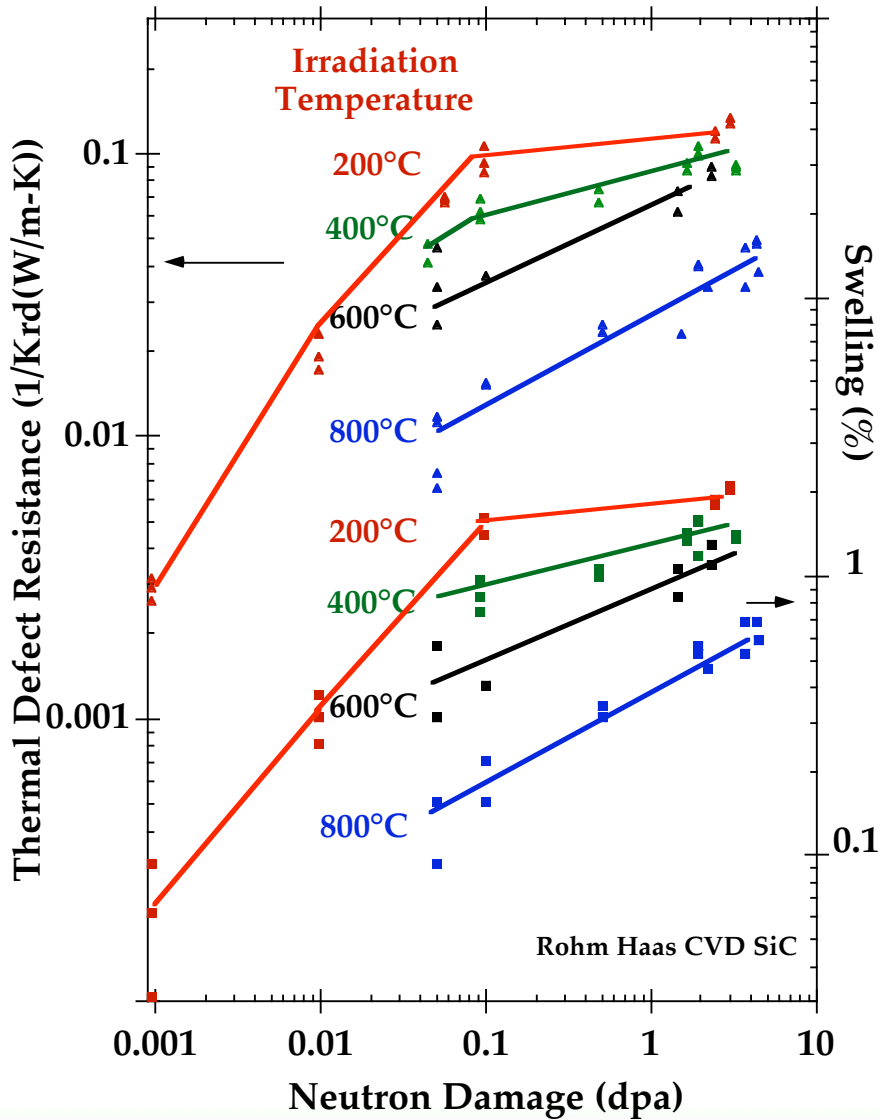
$$\frac{1}{K_{rd}} = \frac{1}{K_{irr}} + \frac{1}{K_{unirr}}$$

Thermal defect resistance due to high vacancy production

$$\frac{1}{K_{rd}} = \frac{6\pi^{1/2}}{k_B} \frac{1}{\omega_D} \left(\frac{\Omega}{aT_m} \right)^{1/2} (C_v T)^{1/2} - \frac{2\pi^2}{k_B} \frac{v^2}{aT_m \omega_D} T$$

The main motivation for using thermal defect resistance is that radiation-induced defects, such as vacancies and clusters, have resistances proportional (or square root dependence) to their concentration and are additive. This gives an easy way to compare stability of ceramics under irradiation.

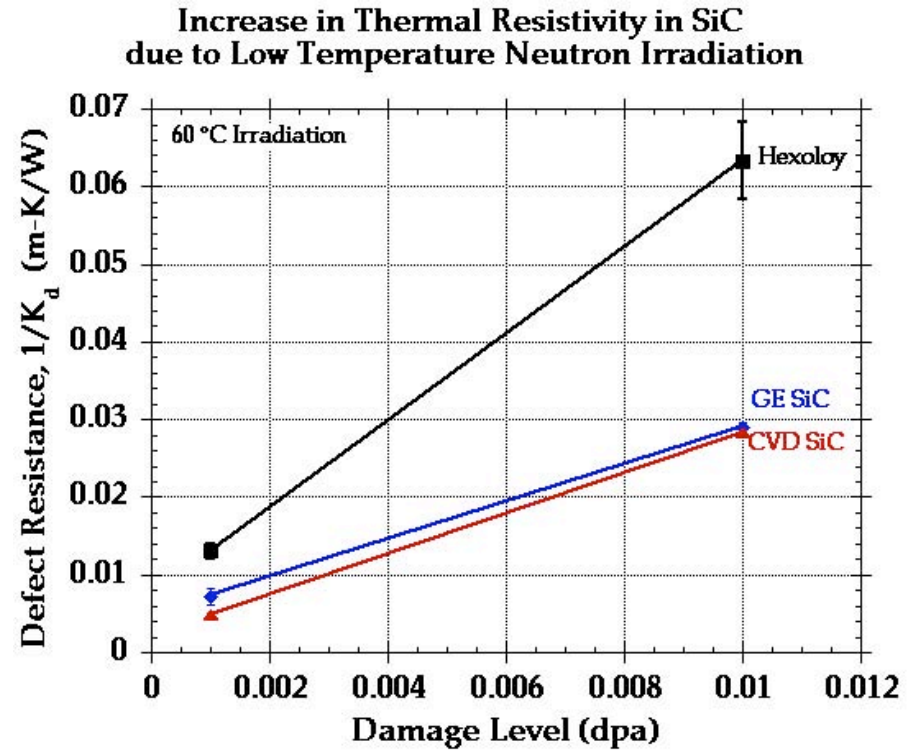
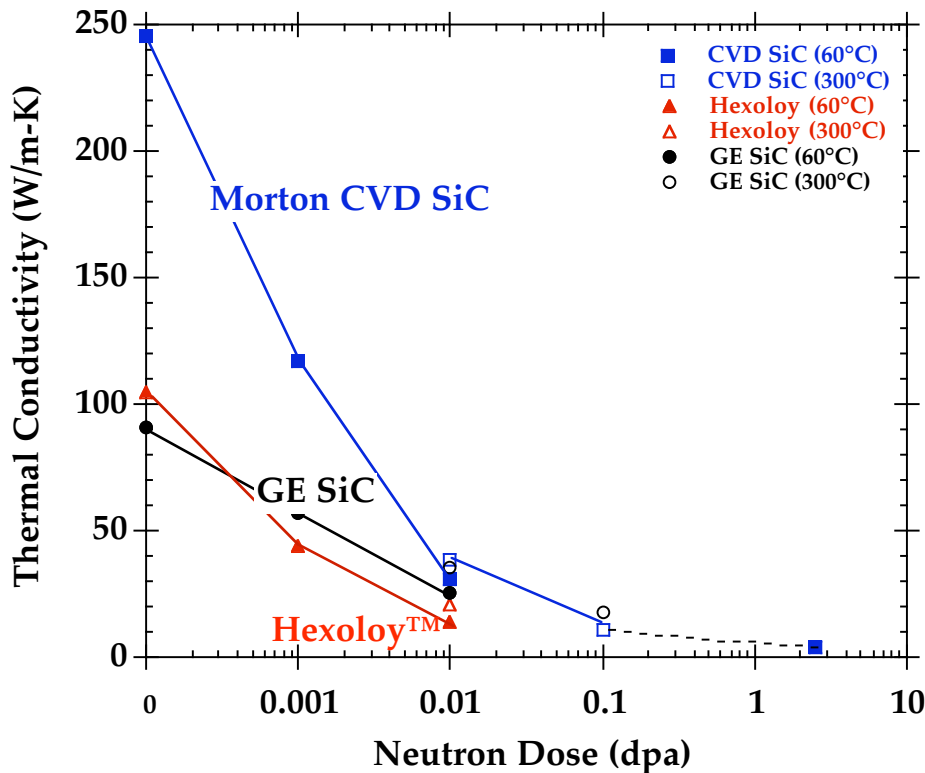
Irradiation-induced Thermal Defect Resistance in Silicon Carbide



Thermal defect resistance normalized to irradiation-induced swelling is constant independent of irradiation temperature (200-800°C) suggesting single defect type controlling phonon scattering

Neutron irradiation-Induced Thermal Defect Resistance of SiC

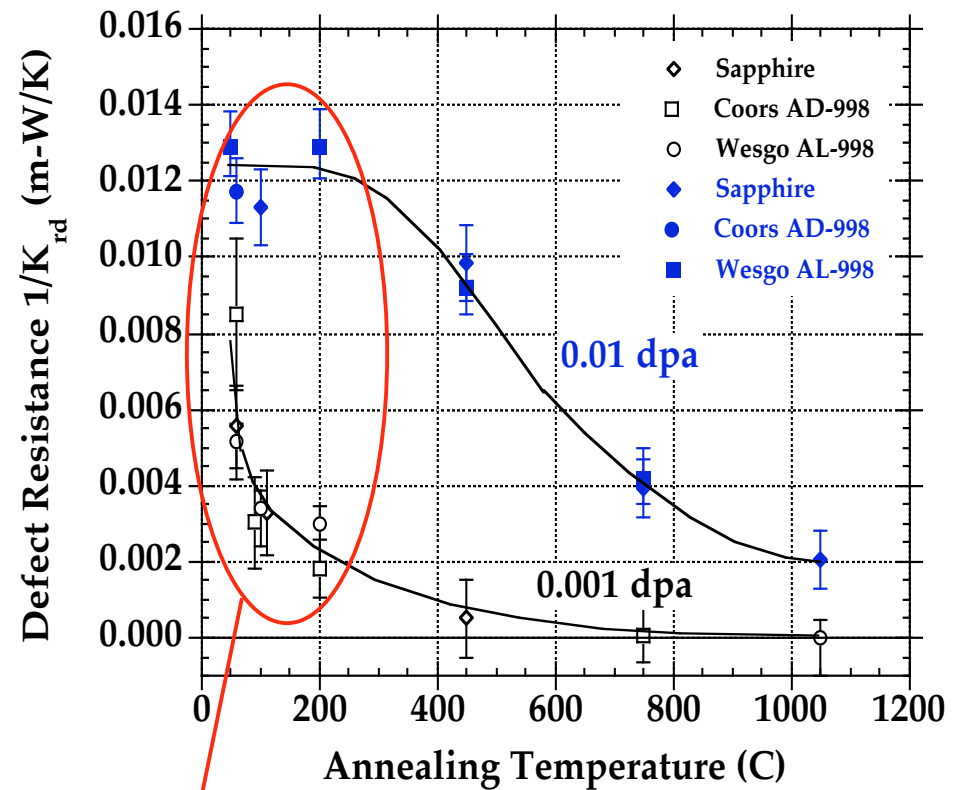
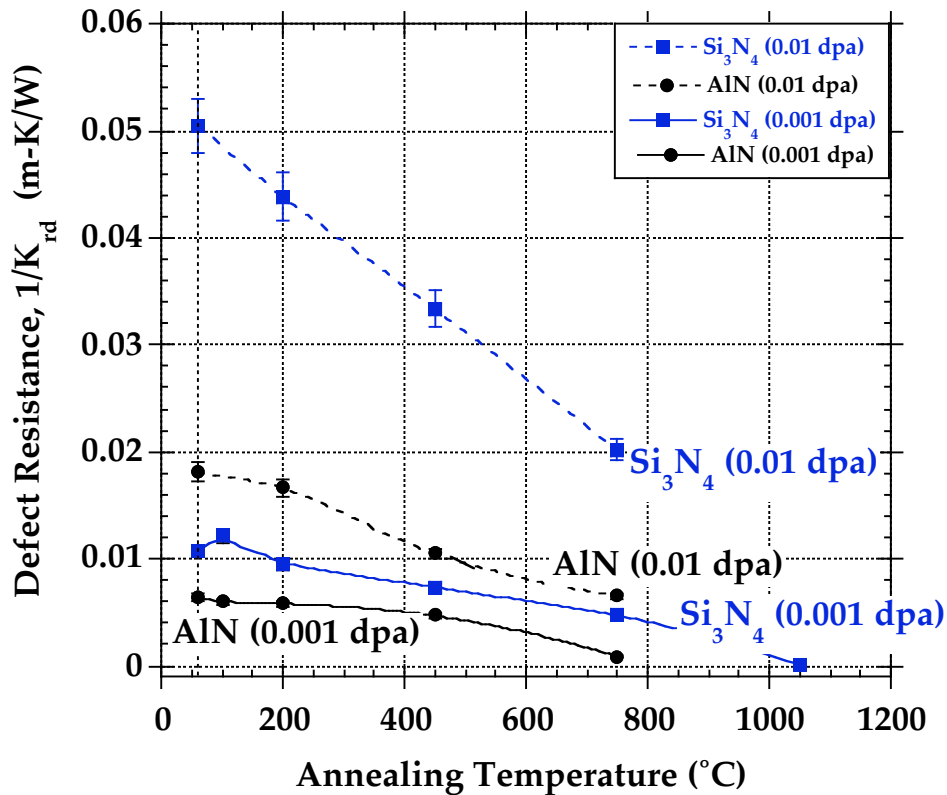
Note thermal conductivity of CVD SiC becomes similar to sintered (GE) SiC after 0.01 dpa



	CVD SiC	GE SiC
Kunirr-Kirr	2.35	0.7
% Kunirr	6%	22%
Defect Resistance	2.8	2.9

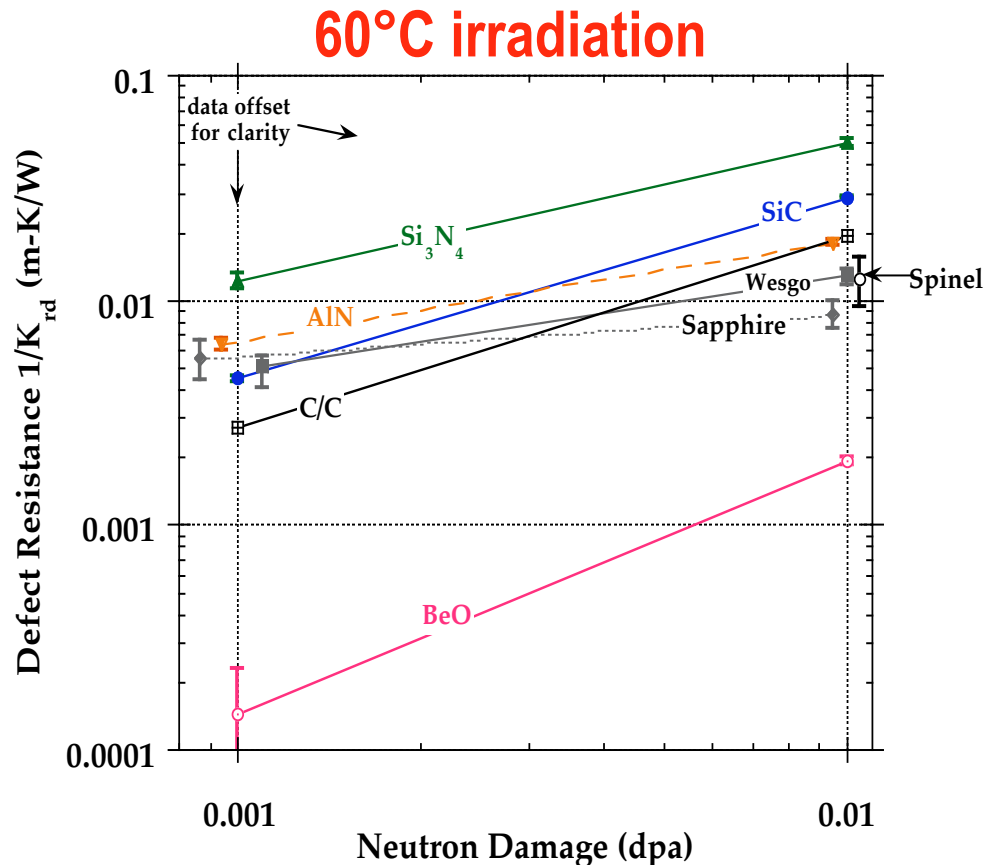
Hexoloy contains boron, which disrupts grain boundary under irradiation. GE SiC and CVD SiC are both high-purity SiC.

Annealing of Radiation-Induced Defects in Oxides and Nitrides



More complex defects formed during higher dose irradiation are more thermally stable.

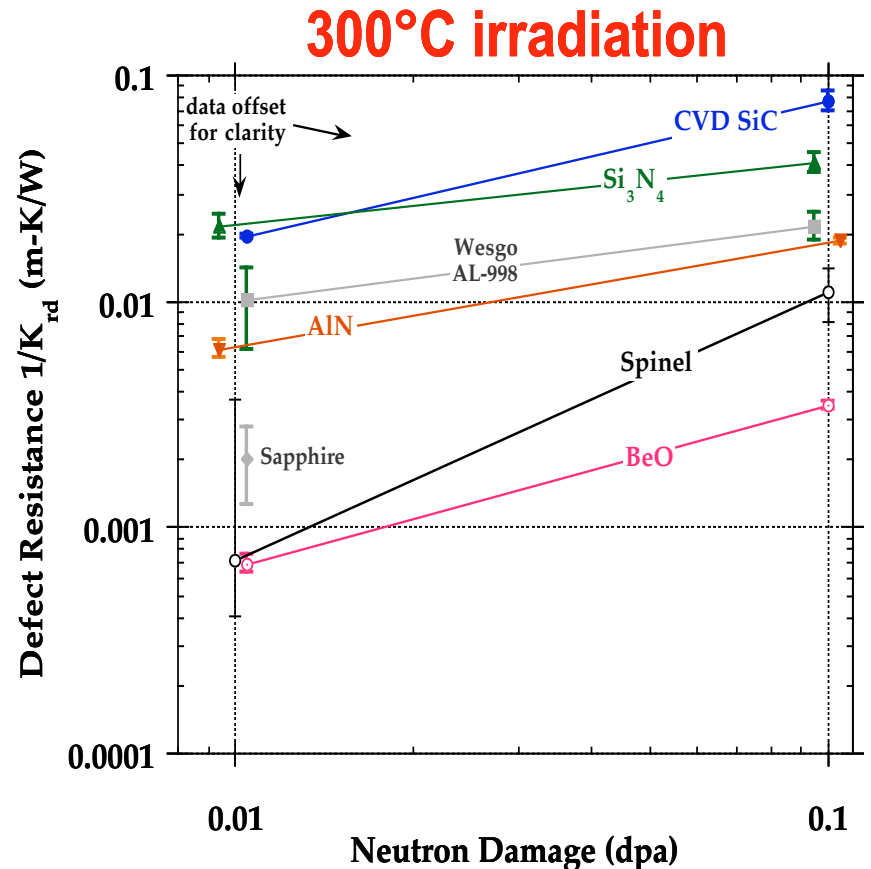
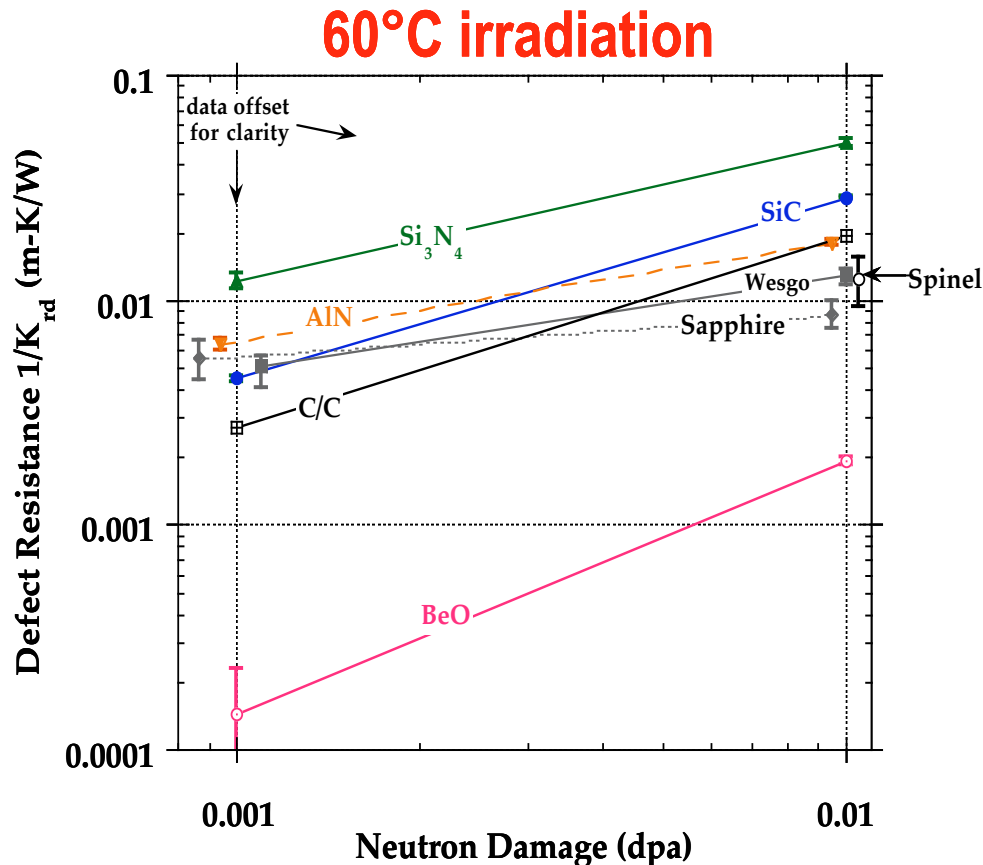
Relative Comparison of Irradiation-Induced Damage



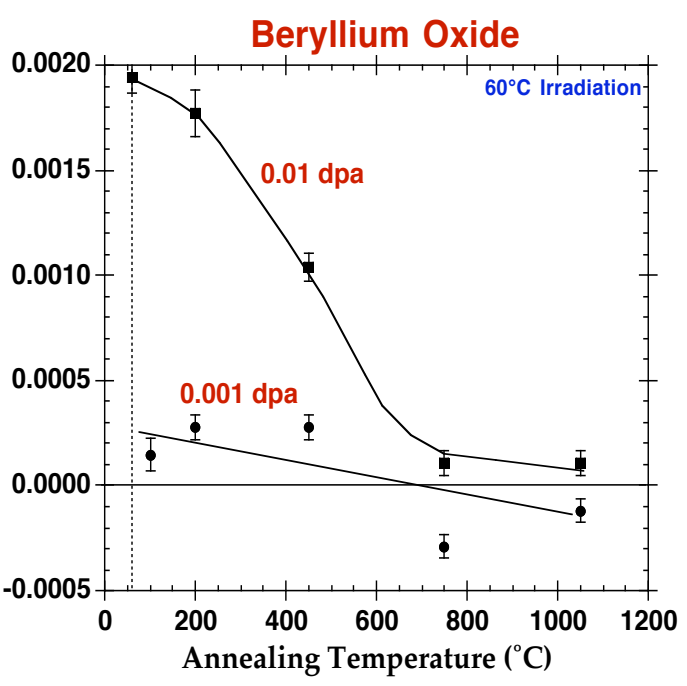
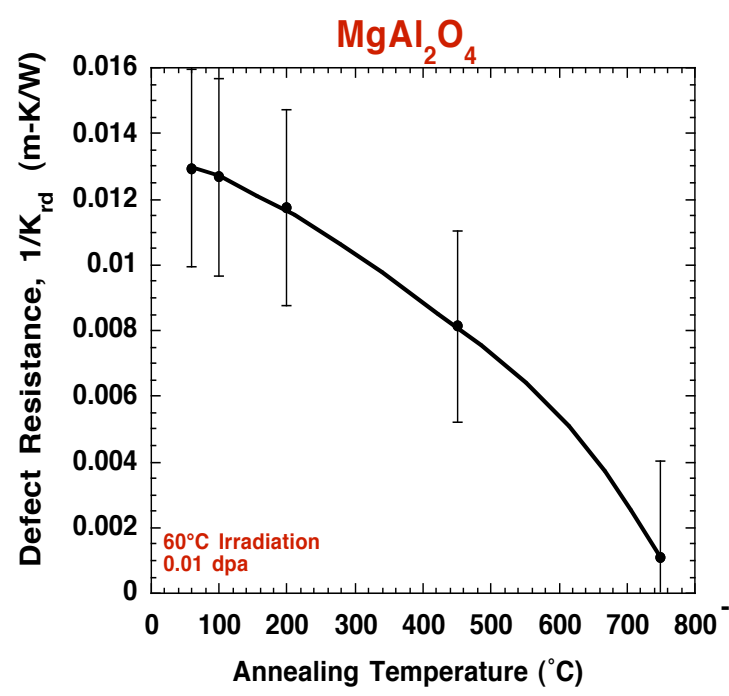
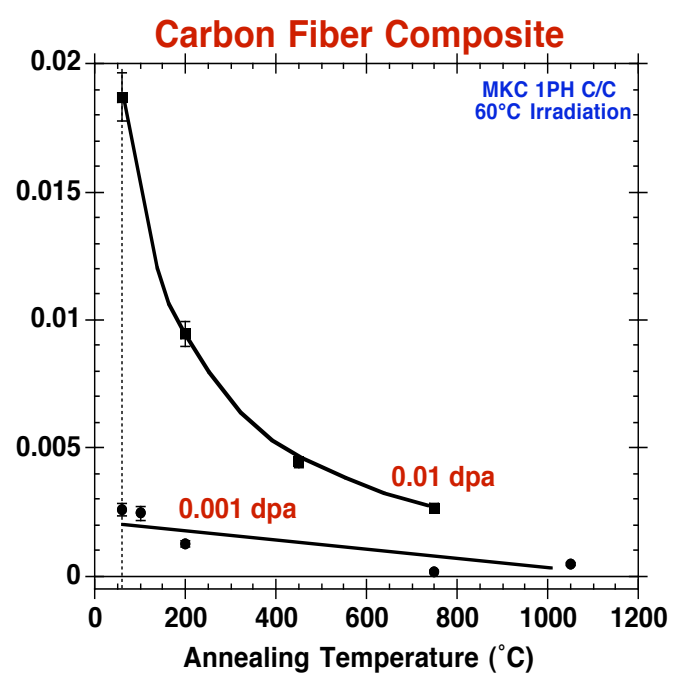
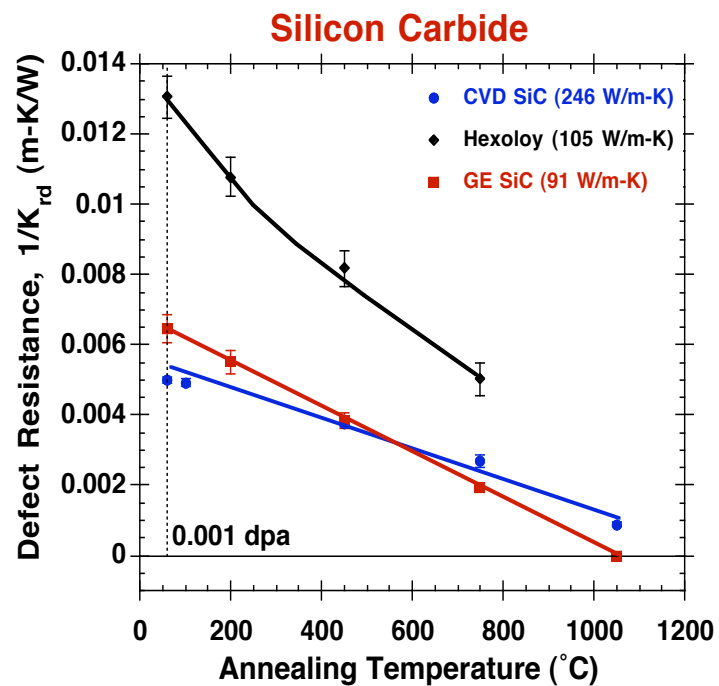
Material	T_{crit} (K)
Al ₂ O ₃	200
AlN	20 < T < 200
BeO	< 120
Graphite	~20
MgAl ₂ O ₄	< 100
SiC	~300
Si ₃ N ₄	< 320

- The susceptibility of the ceramics to thermal conductivity degradation during neutron irradiation at 60°C can be roughly correlated with the available data on observed critical interstitial mobility temperature, where materials with higher interstitial mobility have lower radiation-induced thermal defect resistance and a lower defect resistance accumulation rate $\Delta(1/K_{rd})/\Delta\Phi$.

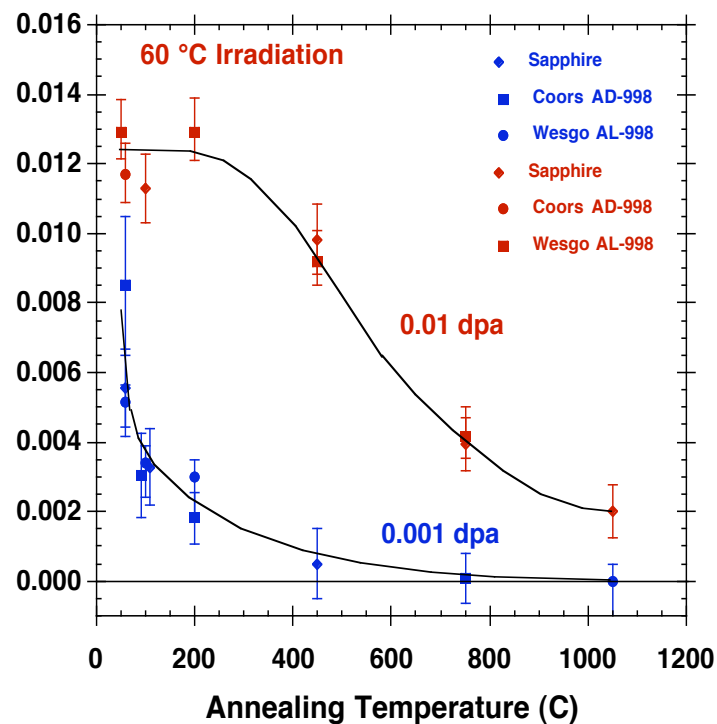
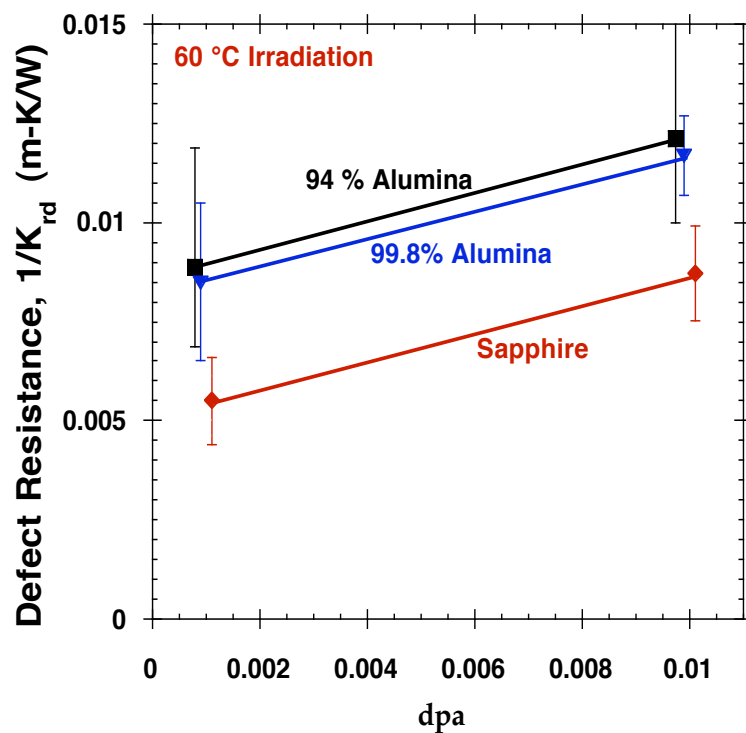
Relative Comparison of Irradiation-Induced Damage



- The defect resistance of all specimens exhibited sublinear dose dependence
- Theoretical analysis for the added thermal defect resistance clearly shows that $1/K_{rd}$ is directly proportional to defect density. Both of these observations indicate that at least some point defects (presumably interstitial type) are mobile in all of these ceramics at the irradiation temperature of 60°C.



Insight into Thermal and Defect Processes



- Resistance is sublinear with dose;
--> $1/K_{rd}$ increases by 2.5 times as dose is increased by 10 times
- Defects are more difficult to anneal as dose is increased.

Insight into Thermal and Defect Processes : Alumina

- $1/K_{rd}$ can be broken into vacancy, loop (and void) terms.

$$\frac{1}{K_{rd\ vac}} = \left(\frac{3\pi}{2K_B}\right)\left(\frac{\omega}{v^2}\right)C_{vac} \quad ; \quad \frac{1}{K_{rd\ loop}} \approx \frac{h^2 R^2 n_{loop}}{K_B}$$

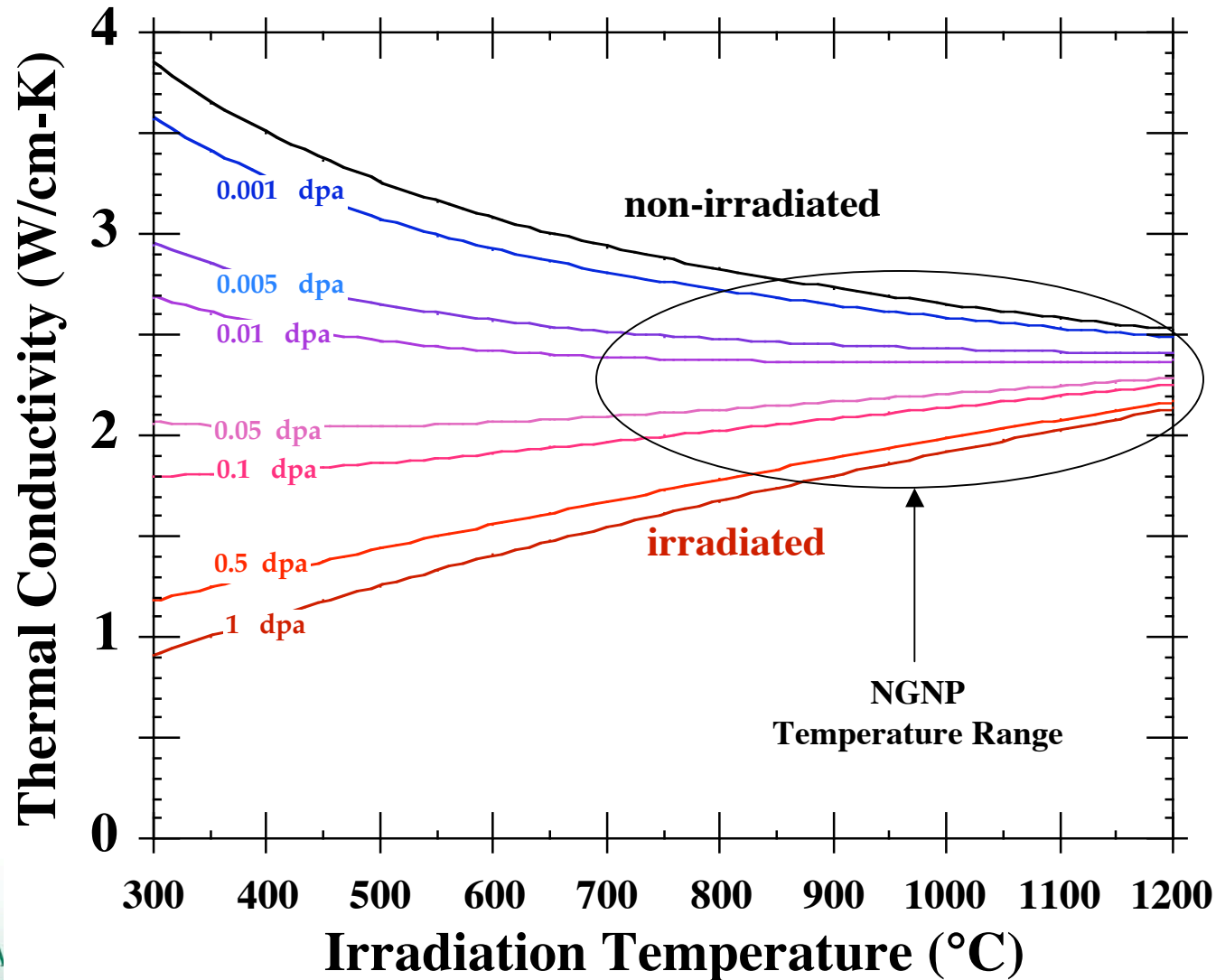
- Following this analysis, **maximum** vacancy concentration can be calculated and compared with optical F-center measurements.

Vacancy (vppm) Concentration	0.001 dpa	0.01 dpa
From $1/K_{rd}$	1000	2000
From F+ Center (Atobe-87)	9	26

- analysis indicates that majority of thermal conductivity degradation in alumina ($T_{irr} = 60^\circ\text{C}$) is due to phonon scattering by loops. This is reinforced by increased difficulty in annealing of defects at higher doses.

Thermal Conductivity Degradation in Carbon Composite

Degradation in High Conductivity Graphite Composite as a Function of Radiation Damage and Temperature



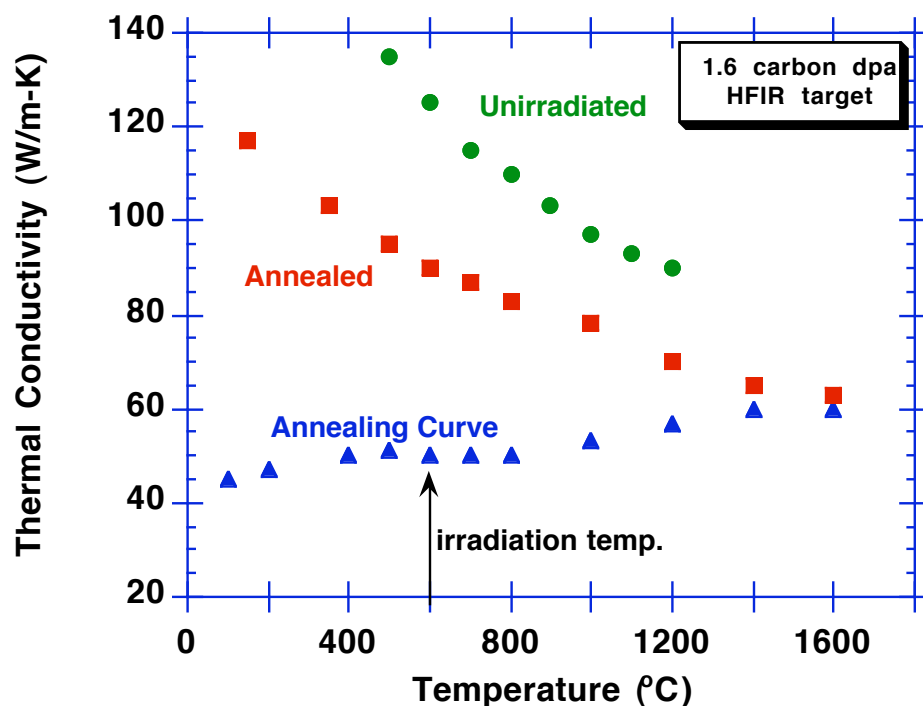
Thermal Conductivity of High Quality Carbon Fiber Composite

$$[K(T)]^{-1} = \left[\frac{1}{K_u(T)} + \frac{1}{K_{gb}(T)} + \frac{1}{K_{d0}} + \frac{1}{K_{rd}} \right]$$

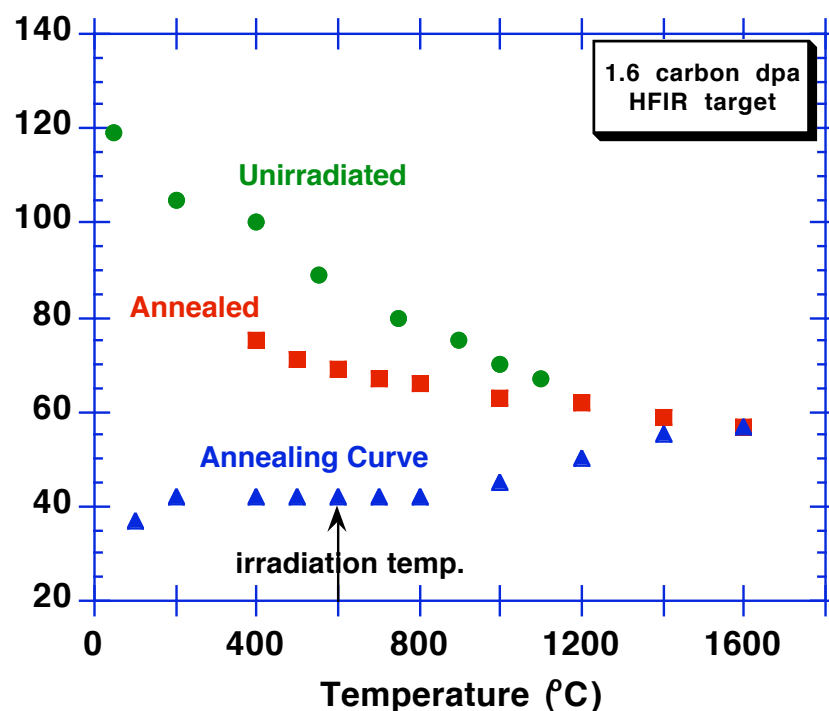
$\frac{1}{K_{rd}}$

 Defect Resistance

Pitch Based C/C Composite

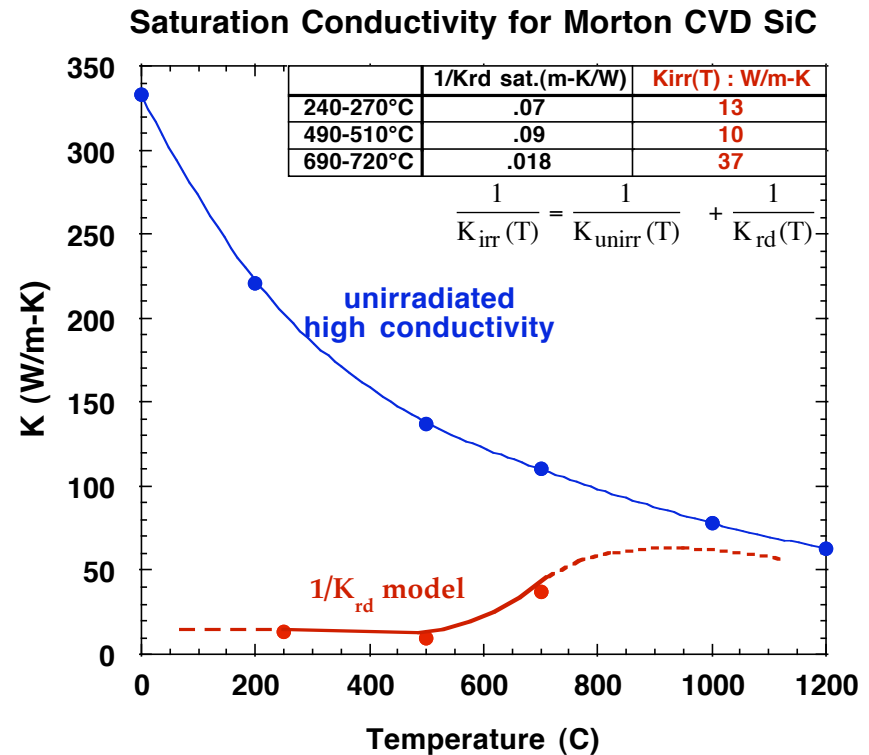
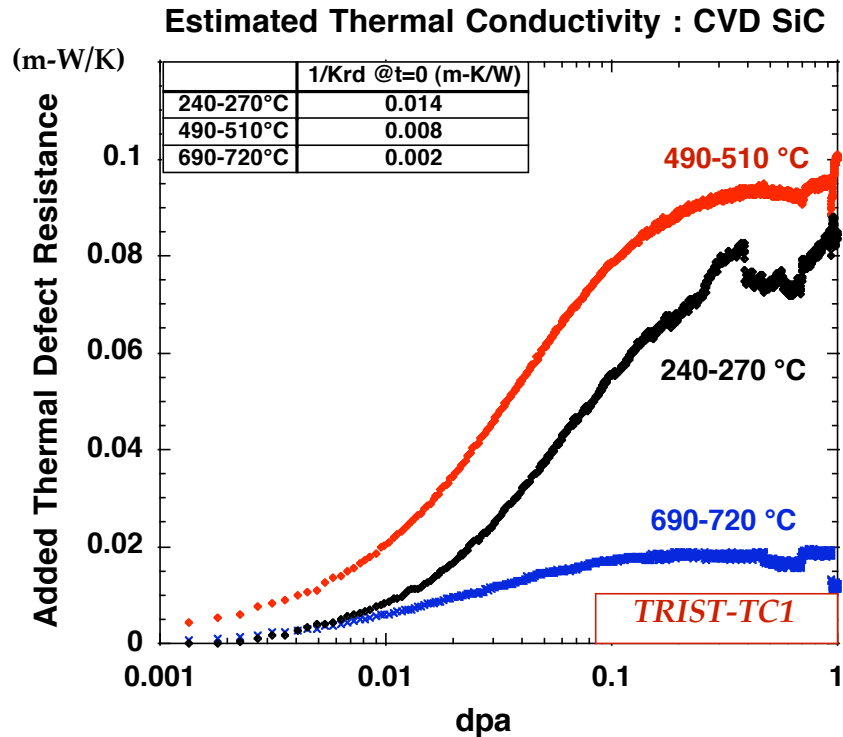


PAN Based Fiber



Defect resistance for PAN and Pitch fibers is identical, despite initial higher unirradiated thermal conductivity of Pitch fibers

Thermal Defect Resistance for Predicting Conductivity



- Maximum thermal conductivity can be estimated for any material based on $1/K_{rd}$ measured from an “ideal” material.
- Maximum irradiated thermal conductivity for SiC is estimated to be ~ 10 W/m-K at 500°C, ~ 37 W/m-K at 700°C.

Summary and Conclusions

- Ionizing radiation can cause large prompt increases in the electrical conductivity of semiconductors and insulators
 - The largest effect occurs in wide band gap insulators
 - Electrical conductivity returns to preirradiation value shortly after irradiation is stopped
 - Radiation induced conductivity (RIC) is a sensitive monitor of ionizing radiation flux, but is not very sensitive to lattice defects
- Many physical properties are sensitive to short range order details (amorphous materials) as well as lattice defects (crystalline materials)
- Changes in thermal conductivity and dielectric properties are sensitive to lattice defects (vacancies and interstitials)
 - Use thermal resistivity to analyze radiation-induced component
 - High unirradiated K_{th} is rapidly reduced during low temperature neutron irradiation
 - In many cases, there is little practical value in using high thermal conductivity ceramics in neutron irradiation environments